AJRCMB Articles in Press. Published on 12-June-2018 as 10.1165/rcmb.2018-0007OC

Lung defense through interleukin-8 carries a cost of chronic lung remodeling and impaired function

Catherine J Reynolds[1,2 †], Kathryn Quigley[1,2 †], Xiaoming Cheng[1], Apurva Suresh[1], Sundas Tahir[1], Fiyyaz Ahmed-Jushuf[1], Khizr Nawab[1], Katherine Choy[2], Simone Alexandra Walker[2], Sara A Mathie[2], Malcolm Sim[1], Janet Stowell[1], Jiten Manji[1], Tracey Pollard[1], Daniel M Altmann[1], Rosemary J Boyton[1,2,3*]

[1]Lung Immunology Group, Infectious Disease and Immunity, Department of Medicine, Imperial College London, W12 ONN UK

[2]MRC & Asthma UK Centre in Allergic Mechanisms of Asthma, UK

[3]Department of Respiratory Medicine, Royal Brompton and Harefield NHS Foundation Trust, SW3 6NP UK

[†]Contributed equally to this study

*Corresponding author and lead contact: r.boyton@imperial.ac.uk (RB). Lung Immunology Group, Infectious Disease and Immunity, Department of Medicine, Room 8N22, Commonwealth Building, Hammersmith Campus, Du Cane Road, Imperial College London, London W12 ONN

Running title: IL-8, lung remodelling and impaired lung function

Copyright © 2018 by the American Thoracic Society

Author contributions: CR, KQ, XC, AS, ST, FA, KN, KC, SW, SM, MS, JS, JM, and TP performed experiments. CR and KQ designed experiments, analysed the data and helped prepare the manuscript. DA interpreted data and helped prepare the manuscript. RB conceived the research, acquired funding, supervised the research, designed experiments, analysed data, interpreted data and wrote the manuscript. All authors read, commented on and agreed the content of the manuscript.

FUNDING: This work was supported by the Medical Research Council (to RB, G108/495), the Welton Foundation (to RB, P14475), the National Institutes of Health–National Institute of Allergy and Infectious Diseases Large Scale T Cell Epitope Discovery Program, Contract HHSN27220090046C (to RB and DA), the National Institute for Health Research Biomedical Research Centre funding scheme (to RB, P46708). KQ was supported by an MRC & Asthma UK Centre, PhD studentship. XC was supported by an Asthma UK project grant (to RB, 05/045). MS was supported by a 4 year Wellcome Trust-NIH PhD studentship (WT095472MA) and JS was supported by a Wellcome Trust Clinician Scientist Fellowship (100046/Z/12/Z). The funders had no role in study design, data collection and analysis, decision to publish, or preparation of the manuscript.

Keywords: interleukin 8, host immunity, bacterial infection, lung function, lung remodelling, tight junction

Copyright © 2018 by the American Thoracic Society

AJRCMB Articles in Press. Published on 12-June-2018 as 10.1165/rcmb.2018-0007OC

Impact on knowledge of the disease process

Long-standing lung expression of IL-8 contributes to a double-edged sword of the inflammatory response in several lung diseases including COPD, bronchiectasis and cystic fibrosis. The IL-8 driven mechanisms underlying these pathologies are poorly understood. The impact of IL-8 on host immunity to bacterial infection and pathogenesis in the lung was modelled through lung targeted transgenic expression of human IL-8. Lung-targeted IL-8 results in enhanced protection from bacterial infection in the lung and drives downstream changes including inflammation, mucus hyper-secretion, lung remodelling and fibrosis, with damaged, leaky, tight junctions and reduced lung function. Thus, IL-8 mediated enhanced microbial immunity comes at a high price of progressive lung damage and reduced lung integrity.

Word count = 110

Copyright © 2018 by the American Thoracic Society

Abstract

Rationale: IL-8 dependent inflammation is a hallmark of host lung innate immunity to bacterial pathogens, yet in many human lung diseases including COPD, bronchiectasis, and pulmonary fibrosis, there are progressive, irreversible pathologic, changes associated with elevated levels of IL-8 in the lung.

Objectives: To better understand the duality of IL-8 dependent host immunity to bacterial infection and lung pathology, we targeted human IL-8 to express transgenically in murine bronchial epithelium, investigating the impact of over-expression on lung bacterial clearance, host immunity, lung pathology and function.

Measurements and main results: Persistent IL-8 expression in bronchial epithelium resulted in neutrophilia, neutrophil maturation, activation and chemtoaxis. There was enhanced protection from challenge with *Pseudomonas aeruginosa* and significant changes in baseline expression of innate and adaptive immunity transcripts for Ccl5, Tlr6, IL2 and Tlr1. There was increased expression of Tbet and Foxp3 in response to the *Pseudomonas* antigen, OprF, indicating a regulatory T cell phenotype. However, this enhanced bacterial immunity comes at the high price of progressive lung remodelling, with increased inflammation, mucus hyper-secretion, and fibrosis. There is increased expression of Ccl3 and reduced expressioh of Claudin 18 and F11r, with damage to epithelial organization leading to leaky tight junctions, all resulting in impaired lung function with reduced compliance, increased resistance and bronchial hyperreactivity measured by whole body plethysmography.

Copyright © 2018 by the American Thoracic Society

AJRCMB Articles in Press. Published on 12-June-2018 as 10.1165/rcmb.2018-0007OC

Conclusions: IL-8 over-expression in the bronchial epithelium benefits lung immunity to bacterial infection, but specifically drives lung damage through persistent inflammation, lung remodelling and damaged tight junctions, leading to impaired lung function.

Word count = 250

Copyright © 2018 by the American Thoracic Society

INTRODUCTION

IL-8 (CXCL8) is a CXC chemokine neutrophil chemoattractant central to innate immunity to bacterial infection (1,2), evidenced by increased susceptibility to infection in defective IL-8 receptor binding (3). Elevated IL-8 is found in the bronchoalveolar lavage (BAL), sputum and lung tissue in chronic lung disease including: chronic obstructive pulmonary disease (COPD), bronchiectasis, cystic fibrosis (CF), idiopathic pulmonary fibrosis (IPF), sarcoidosis, acute respiratory distress syndrome (ARDS) and asthma (4-8). Several of these lung diseases are associated with polymorphisms in the IL-8 gene or its receptors (9-11). Furthermore, increased bronchial IL-8 and neutrophilia contribute to the inflammatory response to exposure to diesel exhaust particles (12).

Generally, raised IL-8 is associated with neutrophilia, the presence of which acutely or chronically, may contribute to significant and often irreversible lung tissue damage (13). However, in addition to persistent neutrophilic inflammation, excessive mucus production, fibrosis and lung tissue remodelling are also common features of many of these diseases. Several key molecules that mediate lung fibrosis also regulate IL-8 expression (14).

IL-8 biological activities are mediated through binding to the G protein-coupled receptors, CXCR1 and CXCR2 (15), found on different immune cell types including neutrophils, monocytes and NK cells as well as on smooth muscle and endothelial cells (16-18). IL-8 receptor ligation activates neutrophil effector mechanisms such as

Copyright © 2018 by the American Thoracic Society

AJRCMB Articles in Press. Published on 12-June-2018 as 10.1165/rcmb.2018-0007OC

degranulation, respiratory burst (19) and neutrophil-independent actions such as in airway smooth muscle migration and function (16, 17,20). In bleomycin-induced fibrosis, CXCR2 receptor blockade reduces fibrosis and collagen deposition through a neutrophil independent mechanism (21). Furthermore, CXCR2 receptor antagonists have been trialled in bacterial challenge models and in clinical settings of lung inflammation including bronchiectasis (22,23).

IL-8 can be produced by diverse cell types including myeloid cells (19). In order to interrogate mechansims underpinning protective and pathogenic roles for persistent IL-8 in lung disease, we generated transgenic mice constitutively expressing human IL-8 (hIL-8) under control of a bronchial epithelial cell specific promoter. Mice lack the gene for IL-8, but the CXCR2 receptor is expressed and can mediate neutrophil chemotaxis upon binding the mouse proteins KC and MIP-2; murine CXCR2 can also bind human IL-8 (24,25). Murine KC is not a direct homologue of human IL-8 (26). We report here the characterization of lung pathology in hIL-8 transgenic mice and show that IL-8 expression in mouse lung mediates neutrophilia, with enhanced neutrophil maturation, activation and chemotaxis, protection from *Pseudomonas* challenge and changes in innate and adaptive immunity transcripts. At the same time it causes lung remodelling, with inflammation, mucus hyper-secretion, fibrosis, and leaky tight junctions, all resulting in impaired lung function; this offers a new model for the study of chronic lung disease.

Copyright © 2018 by the American Thoracic Society

METHODS

Experimental protocols are described in detail in the Supplemental Experimental Procedures.

Mice

Lung targeted hIL-8 transgenics were generated using a construct carrying hIL-8, subcloned into a pBluescript II vector downstream of CC10 promoter and upstream of rabbit β-globin-poly(A) sequence (Supplementary figure 1A). The transgenic founder was backcrossed onto C57BL/6. Mouse experiments were performed within U.K. Home Office legislation under Project License PPL 70/7708.

RT-PCR and real time PCR analysis

RNA was extracted from tissue and cDNA reverse transcribed using SuperScript III.

PCR array

cDNA samples were run on murine innate and adaptive immune response (PAMM-052Z), murine fibrosis (PAMM-120A) or murine tight junction (PAMM-143Z) RT^2 Profiler™ PCR array plates (Qiagen UK) on a Stratagene Mx3000p RT PCR machine. Data was analysed using Partek Genomics Suite version 6.6 (Partek, USA).

Copyright © 2018 by the American Thoracic Society

AJRCMB Articles in Press. Published on 12-June-2018 as 10.1165/rcmb.2018-0007OC

Bronchoalveolar lavage and lung tissue preparation.

BAL fluid and lung tissue were harvested. Snap frozen lung samples were prepared for ELISA by homogenization. Lung was disaggregated. BAL and lung cells were stained by Wright-Giemsa for differential cell counting.

ELISA

Paired antibodies were used for cytokine ELISAs. Albumin concentrations in BAL fluid were determined by ELISA.

Immunohistochemistry

Immunohistochemical staining was performed on wax embedded lung sections using primary antibodies in combination with appropriate biotinylated secondary antibodies. Measurements of smooth muscle diameter around bronchioles and luminal area on SMA stained lung sections were performed. Immunofluorescence staining of Claudin 18 and hIL-8 proteins used rabbit anti-mouse Claudin 18 and goat anti-human IL-8, in combination with donkey anti-rabbit Alexa Fluor® 546 and donkey anti-goat Alexa Fluor® 680. Epithelial/tight junction damage was scored.

Histological scoring of lung inflammation and fibrosis

Sections were stained with Haematoxylin and Eosin (H&E), Periodic Acid-Schiff (PAS) or Masson's Trichrome.

Neutrophil chemotaxis

Copyright © 2018 by the American Thoracic Society

Lung tissue was disaggregated and cells resuspended for chemotaxis assays. Plates were incubated 2.5h and the number of migrated cells quantitated.

Flow cytometry

Neutrophil oxidative burst assays using dihydrorhodamine 123 were performed using PBMCs and lung neutrophils.

***Pseudomonas aeruginosa* infection**

Mice were infected intranasally with $2x10^6$ cfu *P. aeruginosa* (Xen41) and culled for analysis at pre-defined experimental endpoints. The relative quantity of *P. aeruginosa* in lung tissue was determined using primers specific for the *ecfX* gene (27).

T cell assay

Mice were immunized with 25μg OprF in Titermax Gold adjuvant. At d10 draining lymph node cells were harvested for ELISpot or short-term culture with OprF antigen. T cell antigen responses were quantified by IFNγ ELISpot.

Measurement of airway resistance and compliance

Mice were anaesthetized and the trachea cannulated. Resistance and Compliance measurements were taken in an artificial ventilator in response to PBS and increasing doses of methacholine.

Measurement of bronchial hyperreactivity (Penh)

Copyright © 2018 by the American Thoracic Society

AJRCMB Articles in Press. Published on 12-June-2018 as 10.1165/rcmb.2018-0007OC

Measurement of bronchial hyperreactivity was performed by recording respiratory pressure curves by whole body plethysmography.

Isolation of airway smooth muscle cells and Ca^{2+} Flux assays

Smooth muscle cells isolated from lung tissue were incubated with a Fluo-4 dye before stimulation by the rapid addition of calcium ionophore. Baseline measurements were taken and data acquired for at least 5min after stimulation by continuous measurement using a FACSCalibur (BD Biosciences, USA).

Copyright © 2018 by the American Thoracic Society

RESULTS

hIL-8 expression in the lung promotes neutrophilia in transgenic mice

We generated transgenic mice expressing hIL-8 under control of the bronchial epithelial cell specific promoter, Club cell 10 (CC10) (Supplementary Figure 1A). Mice showed hIL-8 transcription limited to the lung, with minor transcription in brain (Supplementary Figure 1B). Immunocytochemistry of lung tissue with antibodies specific for CC10 and hIL-8 showed positive staining limited to bronchial epithelial cells with no hIL-8 expression in alveolar or vascular structures of the lung (Figure 1A). hIL-8 protein was detectable in BAL (Figure 1B), lung homogenate (Figure 1C) and serum (Supplementary Figure 2A) of hIL-8 transgenic mice. There was no significant production of the murine orthologues, *KC* or *MIP-2.* The amount of IL-8 protein produced fell with increasing age as did hIL-8 transcription in the lung (Supplementary Figure 2B and Supplementary Figure 3A-C). In keeping with the function of hIL-8 as a neutrophil chemoattractant (1-2), transgenic mice had increased numbers (Figure 1D) and percent (Figure 1F) of neutrophils in BAL. This was not seen in the lung parenchyma (Figure 1E and 1G) presumed to be because neutrophils recruited to lung tissue move into BAL in response to hIL-8 secretion by the bronchial epithelium.

Having established that lung-targeted expression of hIL-8 results in neutrophilia, the activation status and maturation of neutrophils in the lungs and periphery was investigated. On neutrophil activation, the cell adhesion molecule CD18 is upregulated (28) and degranulation and the respiratory burst processes initiated. H_2O_2 is a major

Copyright © 2018 by the American Thoracic Society

AJRCMB Articles in Press. Published on 12-June-2018 as 10.1165/rcmb.2018-0007OC

product of the neutrophil respiratory burst (29). Neutrophils from the lung tissue of hIL-8 transgenics (but not from peripheral blood) show significantly enhanced production of H_2O_2 (Figure 2A). Expression of the maturation marker Gr-1 and activation marker CD18 was increased on lung and peripheral blood neutrophils from transgenic mice (Figure 2B and 2C). The chemotactic response of lung neutrophils from hIL-8 transgenics to a gradient of recombinant hIL-8 *in vitro* was significantly increased compared to that of neutrophils from wild-type animals (Figure 2D). hIL-8 binds and signals through the CXCR2 receptor on neutrophils resulting in internalisation of the receptor (30). Lower expression levels of the CXCR2 receptor were seen on neutrophils from hIL-8 transgenics (Figure 2E and 2F).

hIL-8 transgenics have improved survival following lung infection with *Pseudomonas aeruginosa*

A pre-activated respiratory niche of mature, activated neutrophils might be considered advantageous in host defence against microbial pathogens. This was investigated in a model of acute lung bacterial infection by *Pseudomonas aeruginosa* (Figure 3). hIL-8 transgenics showed significantly improved protection to acute challenge with $2x10^6$ cfu *P. aeruginosa* (Figure 3A). Seventy per cent of wild-type mice reached the humane end-point within 7 hours of infection compared to just 15% of the hIL-8 transgenic group (p=0.0248). *P. aeruginosa* in lung tissue was quantified 7 hours post-infection in a separate cohort of mice and showed bacterial load to be significantly reduced in the hIL-8 transgenics at this time-point (Figure 3B). No difference in IL-6 was seen between the

Copyright © 2018 by the American Thoracic Society

two groups (Figure 3C), but protection was associated with an enhanced TNFα response and neutrophil infiltration (Figure 3D and 3E).

Chronic hIL-8 expression impacts on innate and adaptive arms of the immune system

Thus far, hIL-8 expression in transgenic mice had been shown to have a pronounced effect on innate, neutrophilic immune pathways at the site of hIL-8 expression and to some extent in the periphery. However, the innate and adaptive arms of the immune system are rarely activated in isolation. A PCR array of relevant genes was analysed in lung tissue from (uninfected) hIL-8 transgenic and wild-type mice (Figure 4A and Supplementary table 1). Transgenic mice showed enhanced transcription of genes involved in chemoattraction and recognition of bacterial lipoproteins such as *Ccl5* and *Tlr6.* In addition, genes associated with adaptive immunity, particularly Th1 responses, such as *Il2, Tbx21,* and *Ifng*, were also up-regulated. *Tlr1* is downregulated.

To investigate T cell responses to bacterial antigen in hIL-8 transgenics, mice were immunized with the *P. aeruginosa* protein outer membrane porin F (OprF). In recall responses to antigen, the number of IFNγ producing cells in the draining lymph node was equivalent between transgenics and wild-types (Figure 4B and 4G). *Tbet* expression was greatly enhanced (Figure 4C). This may be explained by the concomitant up-regulation of other genes, *Foxp3, Il10 and Tgfb1* (Figure 4D, 4H and 4I) associated with a more regulatory phenotype in $Tbet^{+}$Tregs (31,32). There was no evidence for differences in transcription factors or cytokines associated with Th2 or Th17 T cell responses (Figure 4E, 4F and 4J).

Copyright © 2018 by the American Thoracic Society

AJRCMB Articles in Press. Published on 12-June-2018 as 10.1165/rcmb.2018-0007OC

Lung inflammation, mucus hyper-secretion and fibrosis

From the infection studies, it was clear that hIL-8 transgenics display enhanced lung host defence. Investigation turned to whether long-standing exposure to hIL-8 would result in pathological changes in lung classically observed in human chronic lung diseases. Histological comparison of (uninfected) mice showed inflammation around bronchi and blood vessels (Figure 5A) accompanied by increased transcription of *Muc5b* and *Muc5ac,* the major mucin protein components of airway mucus (33). These were increased 6-fold and 10-fold respectively (Figure 5B and 5C). Excessive mucus production is a pathological feature of many chronic lung diseases, including asthma, COPD, bronchiectasis and CF (34). Mucus-hypersecretion, as evidenced by PAS staining, was frequently observed in transgenic lung tissue and co-localised to areas of the bronchial epithelium with the greatest production of hIL-8 protein (Figure 5D). This was not seen in wild-type mouse lung.

We next investigated another key pathological feature, lung fibrosis, using Masson's Trichrome staining of lung tissue (Figure 5E). Fibrotic changes, as measured by Ashcroft scoring, were more apparent in lung tissue from hIL-8 transgenic mice than controls in older mice (>27 weeks). Transcriptional analysis showed increased expression of transcripts for the extracellular matrix proteins collagen I and collagen III (Figure 5F and 5G) with a significant difference between transgenics and controls seen for expression of collagen III ($p=0.0039$). Further evidence that fibrotic processes occurred in the lungs of older hIL-8 transgenics came from a transcriptional array of

Copyright © 2018 by the American Thoracic Society

fibrotic genes in lung tissue of 20 week old mice (Figure 5H and Supplementary table 2). Key genes in fibrotic pathways, such as *Ifng, Ccl3, Il1b, Sp1, Tgfbr 1* and *Tgfbr 2,* were up-regulated in hIL-8 transgenics as was *Cxcr4*, which is chemotactic for lymphocytes. *Timp1*, a metalloproteinase inhibitor, was downregulated. Increased transcription of *Ccl3* is apparent in hIL-8 transgenic lung from 20 weeks of age, whilst differences in *Ifng* transcription are present from as early as 10 weeks (Figure 5I and 5J). Increased levels of CCL3 and IFNγ protein was present in homogenized lung tissue (Figure 5K and 5L).

Lung remodelling leads to reduced lung function

A major physiological consequence of irreversible structural damage to the airways is reduced lung function. We hypothesized that the lung inflammation, mucus hyper-secretion and fibrosis observed in the lungs of hIL-8 transgenic mice would negatively impact on lung function parameters such as airway resistance and compliance. We observed increased airway resistance and reduced lung compliance in hIL-8 transgenics in response to methacholine challenge (Figure 6A and 6B). There was evidence of increased, bronchial hyper-reactivity in older mice (<18 compared to >42 weeks of age), measured by Penh (Figure 6C).

The changes in lung function did not result from increased smooth muscle mass, a feature of airway remodelling postulated to contribute to abnormal lung resistance in diseases such as COPD and asthma (35). Expression of α-smooth muscle actin (α-SMA) was not significantly increased in the lung tissue of hIL-8 transgenics (Figure 6D).

Copyright © 2018 by the American Thoracic Society

AJRCMB Articles in Press. Published on 12-June-2018 as 10.1165/rcmb.2018-0007OC

Nor did lung function changes result from major differences in smooth muscle function, as primary smooth muscle cells from transgenics and wild-type control mice showed similar magnitude and kinetics of calcium flux in response to stimulus (Figure 6E). Immunocytochemistry of lung sections from hIL-8 transgenic and wild-type animals showed no difference in thickness of α-SMA surrounding the bronchi (Figure 6F). The luminal area of airways in transgenic mice was smaller than those of control mice (Figure 6G).

α-SMA, along with collagen I and collagen III are markers for epithelial to mesenchymal transition (EMT) (36), a pro-fibrotic process believed to play a role in the pathogenesis of several lung diseases including COPD (37). Hallmark EMT comprises down-regulation of epithelial transcripts such as E-cadherin and occludin, with up-regulation of mesenchymal transcripts such as vimentin and fibronectin. There was no significant E-cadherin down-regulation in lungs of hIL-8 transgenics, although occludin transcription was reduced 2-fold in older mice (Figure 6H and 6I). Neither vimentin nor fibronectin were up-regulated; fibronectin transcripts were significantly reduced (Figure 6J and 6K). Taken together, the data suggest that long-standing hIL-8 exposure results a reduction in lung function, but are not related to changes in smooth muscle or a consequence of a classic EMT program.

Longstanding hIL-8 exposure results in disruption of tight junction integrity

Although data thus far did not support a role for EMT in lung remodelling, significant down-regulation of transcripts for occludin and fibronectin were observed. Occludin is a

Copyright © 2018 by the American Thoracic Society

key protein of epithelial tight junctions (Figure 7A) which play a vital role in maintaining the barrier function of the epithelium and its integrity. Disruption of epithelium integrity is suggested to be compromised in lung diseases such as CF (38). Fibronectin is a component of the extracellular matrix important in promoting the formation of these barrier complexes (39). Transcripts for other tight junction proteins Claudin 18, Jam1 and ZO-1 were down-regulated in hIL-8 transgenic mice compared to controls (Figure 7B, 7C and 7D), particularly in older mice (>27 weeks). A gene array identified reduced transcription of additional tight junction proteins such as *Magi3, Jam2 and Cgn* (Supplementary table 3) and upregulated transcription of *Cldn4,* shown to be protective in acute lung injury (40). The data suggests that the integrity of lung epithelial tight junctions might be compromised. The possibility of tight junction disruption was investigated by immunocytochemistry of lung epithelium from older mice and showed considerable damage to epithelial cell organisation, junctions and polarity with a significantly increased epithelial damage score (Figure 7E and 7F). This effect was not seen in epithelium from other tissues not expressing the IL-8 transgene. Disrupted organization of epithelial tight junctions correlated closely with IL-8 expression (Figure 7E). Lung epithelial damage correlated with functional impairment of tight junction permeability, since BAL albumin concentration was increased 5-fold in hIL-8 transgenics (Figure 7G). Collectively these data suggest that long-standing exposure of lung tissue to hIL-8 activates inflammatory and regulatory processes, which over time result in damage to the bronchial epithelium, including loss of tight junction integrity, and causes long-term and irreversible lung remodelling with concomitant decline in lung function.

Copyright © 2018 by the American Thoracic Society

AJRCMB Articles in Press. Published on 12-June-2018 as 10.1165/rcmb.2018-0007OC

DISCUSSION

We have characterized the impact of long-standing expression of high levels of hIL-8 protein in murine lung. We demonstrate neutrophilia and protection from bacterial challenge, but also that enhanced immunity comes at the cost of chronic inflammation with evidence of damage to the integrity of the bronchial epithelium, lung remodelling processes and a decline in lung function.

It is a given that the IL-8/CXCR2 axis for neutrophil recruitment is first line innate defence for respiratory host immunity to bacterial and fungal pathogens. For example, a raised acute phase IL-8 response features in pneumococcal pneumonia (41). However, potent respiratory IL-8-mediated immunity is a double-edged sword, illustrated by the number of chronic inflammatory lung diseases encompassing elevated local IL-8, including CF, COPD, IPF, bronchiectasis, sarcoidosis, ARDS and asthma (4-8). There have been previous attempts to explore specific functions of IL-8 or its murine homologue, KC, through targeted expression in transgenic strains or through administration of recombinant cytokines (26,42,43). Wan *et al* showed increased lung bacterial clearance and improved survival following infection with *Klebsiella pneumoniae* in a transgenic expressing lung targeted KC (42). This was associated with polymorphonuclear leukocyte trafficking to the lung. hIL-8 gene expression in our model is confined to the bronchial epithelium, an important physiological source of this cytokine in the human lung (44). The levels of hIL-8 protein reported here (range 5,891 to 39,466 pg/ml) in the mouse BAL fluid are significant. High hIL-8 levels have been reported in the literature for patients with COPD (250–750pg/ml), CF (3800 pg/ml) and

Copyright © 2018 by the American Thoracic Society

asthma (30 pg/ml) (4,45,46). However, hIL-8 is a less potent chemoattractant for murine neutrophils than for human cells (25) and it is difficult to make direct comparisions between BAL hIL-8 levels found in the transgenic mice with those of COPD patients.

We have shown that recruitment of mature and activated neutrophils into the airways of hIL-8 transgenic mice confers protection from acute *P. aeruginosa* infection. Persistent *P. aeruginosa* infection is a major problem in bronchiectasis and CF and the key role for neutrophils in the innate immune response to this pathogen is well described (47,48). Neutrophils are an important source of pro-inflammatory IL-1β during acute *P. aeruginosa* pneumonia (49). We here report up-regulation of IL-1β transcripts in the lungs of older hIL-8 transgenic mice. The documented actions of IL-1β in driving lung fibrotic processes (50) serve as a possible link between expression of hIL-8 and the lung remodelling and fibrosis seen in our mice. Other pro-fibrotic proteins up-regulated in the hIL-8 transgenic lung that can be secreted by activated neutrophils include IFNγ and CCL3 (51,52). Although the specific cellular source of gene expression is not known as these studies were carried out using RNA made from whole lung. CCL3 is only elevated in the lung tissue of older mice while IFNγ transcripts are increased in mice as young as 10 weeks. Both are probably contributing towards the inflammatory response, fibrosis and remodelling observed in these mice. Studies showing IFNγ has a negative effect on tight junction integrity (38) demonstrate the inter-relatedness of these pathologies.

Copyright © 2018 by the American Thoracic Society

AJRCMB Articles in Press. Published on 12-June-2018 as 10.1165/rcmb.2018-0007OC

While it is possible that the source of increased IFNγ in our model is activated neutrophils, the observation that the archetypal Th1 cell transcription factor, *Tbet*, is also up-regulated, suggests that hIL-8 expression is also triggering adaptive immune pathways. Neutrophils lie within the innate arm of the immune system, but other studies have highlighted their potential as antigen presenting cells for T cell activation (53). It is also possible that production of reactive oxygen species by activated neutrophils results in collateral damage to the lung mucosa, or that loss of tight junction integrity exposes antigens capable of triggering an adaptive T cell response. Our data looking at T cell immunity to the *P. aeruginosa* antigen OprF shows that regulatory mechanisms of the adaptive immune system have also been engaged in the hIL-8 transgenics, presumably as a consequence of long-term exposure to pro-inflammatory signals such as IFNγ. Induction of *Foxp3* and anti-inflammatory cytokines *Il10* and *Tgfb1* meant that over-activation of Th1 immunity may be partially counter-balanced. In addition to *Tgfb1* up-regulation in T cells, lung tissue from hIL-8 transgenic mice was shown to have increased levels of TGF-β receptors *Tgfbr1* and *Tgfbr2.* It is not surprising that regulatory mechanisms including those elicited through TGF-β signalling should be up-regulated in a situation where the inflammatory trigger namely hIL-8 is continuously present. This will also be the case in patients with chronic lung diseases such as COPD, bronchiectasis, and CF where underlying factors pre-dispose to repeated bacterial infection. The caveat to controlling inflammation through anti-inflammatory mechanisms such as TGF-β signalling is that these mechanisms are also potent inducers of tissue fibrosis. Disruption of epithelial tight junctions in hIL-8 transgenics was profound, apparent in significant leakage of albumin into the BAL.

Copyright © 2018 by the American Thoracic Society

The data presented here provide insight into the consequences of long-term exposure to hIL-8 in the lung. IL-8 is an integral component of innate immunity to infection and as such, overexpression is beneficial in combating bacterial infection. However, if levels of IL-8 are elevated over a long time-scale, the resultant inflammatory cascades initiated and consequent anti-inflammatory and regulatory mechanisms that are deployed culminate in long-term structural damage to the tissue, with inflammation, mucus hyper-secretion, remodelling, damaged and leaky epithelial tight junctions and fibrosis all leading to reduced lung function. For patients suffering from chronic lung disease associated with elevated IL-8, therapeutic intervention to temper excessive pro-inflammatory effects may be beneficial.

Copyright © 2018 by the American Thoracic Society

AJRCMB Articles in Press. Published on 12-June-2018 as 10.1165/rcmb.2018-0007OC

ACKNOWLEDGEMENTS

The authors acknowledge the MRC & Asthma UK Centre in Allergic Mechanisms of Asthma, UK and Professor Clare Lloyd for support with lung function studies. The authors acknowledge the support of NIHR Imperial BRC multi-parameter flow cytometry and confocal imaging facility, Hammersmith Campus, Imperial College London. The authors acknowledge the support of the Transgenics and Embryonic Stem Cell Facility, MRC London Institute of Medical Sciences and Central Biomedical Services at the South Kensington and Hammersmith Campus, Imperial College London. The authors wish to thank Dr Michael Poidinger for his help and advice with the bioinformatic analysis. We thank Michael Spencer for help with T cell studies. The authors thank Professor Jeffery Whitsett for providing the CC10 promoter and Dr Helen Bodmer for supplying the rabbit β-globin poly (A) cassette. The authors thank Amarjit Naura and Hamid Boulares for sharing their protocols relating to the isolation and culture of primary smooth muscle cells from mouse lung.

COMPETING INTERESTS

The authors declared that there are no financial, personal, or professional competing interests that could be construed to have influenced the work. The authors declare that they do not have any related or duplicate manuscript under consideration (or accepted) for publication elsewhere

Copyright © 2018 by the American Thoracic Society

FIGURE LEGENDS

Figure 1. Expression of hIL-8 in transgenic mice is localised to the bronchial epithelium and is associated with recruitment of neutrophils into the airways. (A) Localisation of hIL-8 protein in the bronchial epithelium of the lung was established by immunohistochemical staining for hIL-8 and CC10 in consecutive paraffin embedded lung sections (x20 magnification). Levels of hIL-8 protein and the murine orthologs KC and MIP-2 were determined by ELISA in (B) BAL fluid and (C) homogenised lung samples of hIL-8 transgenic mice [aged 8 weeks (n=7), 11 weeks (n=6), 24 weeks (n=2) and 34 weeks (n=3)] and in a cohort of wild-type mice aged 11-34 weeks (n=13). The total numbers of neutrophils and the neutrophil percentage in BAL (D and F) and lung (E and G) was determined by differential cell counting of Wright-Giemsa stained cytospins. Error bars represent mean $\pm$ SEM. Statistical significance was determined using an unpaired t-test (*$p<0.05$, **$p<0.005$, ***$p<0.0005$, ****$p<0.0001$).

Figure 2. Neutrophils in the lungs of hIL-8 transgenic mice are more mature, more activated and more chemotactic to rhIL-8. (A) NADPH oxidase activity in neutrophils from the lung and peripheral blood of hIL-8 transgenic (n=10, black squares) and wild-type mice (n=6, black circles) aged 15-18 weeks was measured using a DHR assay. Expression of the neutrophil maturation marker GR-1 (B) and the neutrophil activation marker CD18 (C) were measured by flow cytometry. (D) Lung neutrophils from hIL-8 transgenics (n=5, black squares) showed an enhanced chemotactic response to rhIL-8 *in vitro* compared to cells from wild-type animals (n=4, black circles) [mice aged 26-37 weeks]. (E and F) Flow cytometry showed cell surface expression of the hIL-8 receptor,

Copyright © 2018 by the American Thoracic Society

AJRCMB Articles in Press. Published on 12-June-2018 as 10.1165/rcmb.2018-0007OC

CXCR2, on lung neutrophils from hIL-8 transgenics (n=6, black squares) compared to wild-types (n=6, black circles) [mice aged 9-15 weeks]. Error bars represent mean±SEM. Statistical significance was determined using an unpaired t-test (*p<0.05, **p<0.005, ***p<0.0005).

Figure 3. Lung expression of hIL-8 in transgenic mice confers protection from infection with *Pseudomonas aeruginosa.* (A) 8-10 week old hIL-8 transgenic (black squares) and wild-type control mice (black circles) (n=7 per group) were infected intranasally with $2x10^6$ CFU *P. aeruginosa* (PA) and disease severity monitored over a 32h period. A separate cohort of 13-14 week old mice (n=5 per group) were sacrificed at 6h post infection and relative quantity of PA present in the lung tissue determined by rtPCR (B). 8 week old hIL-8 transgenic (black bars) and wild-type mice (white bars) were given $2x10^6$ CFU *P. aeruginosa* (n=6 per group) or PBS (n=5 per group) intranasally and culled at 6h post infection (C) TNFα and (D) IL-6 concentrations in BAL fluid were determined by ELISA. (E) Total BAL inflammatory cell counts were determined using Wright-Giemsa stained cytospins. Numbers of macrophages (striped bars), neutrophils (grey bars) and lymphocytes (checked bars) are shown. Error bars represent mean±SEM. Statistical significance was determined using the Log-Rank (Mantel-Cox) test for disease severity curves and an unpaired t test for all other data (*p<0.05, **p<0.005).

Figure 4. Expression of hIL-8 in the lung is associated with transcriptional changes in adaptive and innate immune related genes. (A) Lung RNA was isolated from hIL-8 transgenic (n=5) and wild-type mice (n=5) 20 weeks of age. An SA

Copyright © 2018 by the American Thoracic Society

Biosciences innate and adaptive immune system PCR array was run for all samples. A heat map shows gene expression that was statistically different ($p<0.05$) between the two groups with a fold change of $\pm$1.2 and above. A colour scale is used to represent a fold increase (red) and a fold decrease in gene expression (blue). Statistical significance was determined using a one-way ANOVA. Data shown are all genes that were statistically different with a fold change greater than 1.2 and $p<0.05$. To interrogate differences in adaptive immune responses between transgenic and wild-type mice, 8-9 week old hIL-8 transgenics (n=12, black squares) and wild-type mice (n=5, black circles) were primed sub-cutaneously in the footpad with *P. aeruginosa* antigen OprF, in combination with Titermax adjuvant. Ten days post-immunisation, the draining popliteal lymph node (DLN) and spleen were removed. (B) hIL-8 transgenic (black squares) and wild-type (black circles) $CD4^+$ T cell responses to OprF from both DLN (i) and spleen (ii) were assayed by IFNγ ELISpot. DLN and spleen cells from hIL-8 transgenic (black bars) and wild-type animals (white bars) were additionally cultured with 25 μg/ml of OprF for 3d before cell lysis for real time PCR analysis of (C) *Tbet*, (D) *Foxp3*, (E) *Gata3* and (F) *RORγt,* (G) *Ifng,* (H) *IL-10,* (I) *Tgfb1* and (J) *IL-17A* transcripts. Error bars represent mean ± SEM. Statistical significance was determined using an unpaired t-test (*$p<0.05$, **$p<0.005$).

Figure 5. Expression of hIL-8 in lung associated with inflammation, mucus hypersecretion and fibrosis. (A) A validated scoring system for bronchi and blood vessels was used to assess levels of inflammation in H+E stained paraffin lung sections from hIL-8 transgenic (n=40, black bars, 10-29 week old) and wild-type mice (n=22,

Copyright © 2018 by the American Thoracic Society

AJRCMB Articles in Press. Published on 12-June-2018 as 10.1165/rcmb.2018-0007OC

white bars, 10-20 week old). A representative image from each group is shown (x20 magnification). Relative expression levels of mucin genes (B) *Muc5b* and (C) *Muc5ac* in lung tissue from hIL-8 transgenic (n=27, 10-30 week old) and wild-type mice (n=13, 10-30 week old) were determined by rtPCR (D) Periodic Acid-Schiff (PAS) staining for mucus was co-localised with immunohistochemical staining for hIL-8 using consecutive paraffin embedded lung sections (x40 magnification). (E) The Ashcroft score system was used to measure degree of fibrosis in Masson's Trichrome stained lung tissue from hIL-8 transgenic and wild-type mice aged from 10 to 27 weeks (n=9 to 18 per group). Representative images are shown (x20 magnification). Relative expression levels of the fibrotic markers (F) *Col1A1* and (G) *Col3A1* were measured by rtPCR (n=17 hIL-8 transgenic and n=13 wild-type mice aged 11-30 weeks old). (H) A PCR array of genes implicated in fibrotic pathways was performed on lung RNA isolated from 20 week old hIL-8 (n=5) and wild-type (n=5) animals. The heat map shows genes with a fold change of $\pm$1.2 and above where $p<0.05$. Statistical significance was determined using a one-way ANOVA. (I) *Ccl3* and (J) *Ifng* transcripts were compared in lung tissue from hIL-8 transgenic and wild-type mice at (i) 10 weeks, (ii) 20 weeks and (iii) 27 weeks of age (n=5 per group). (K) CCL3 and (L) IFNγ protein levels were also measured in homogenised lung tissue from 20 week old mice. Error bars represent mean±SEM. Statistical significance was determined using an unpaired t-test (*$p<0.05$, **$p<0.005$, ***$p<0.0005$).

Figure 6. Chronic IL-8 exposure results in impaired lung function with increased airway resistance and reduced compliance. The lung function parameters of airway

Copyright © 2018 by the American Thoracic Society

(A) resistance and (B) compliance were measured in 12 to 15 week old hIL-8 transgenic (n=8, black squares) and wild-type (n=6, black circles) animals. (C) Penh was measured in hIL-8 transgenic mice of different ages, a younger age group aged 9-12 weeks (n=8, black triangles) and an older age group aged 41-44 weeks (n=4, black diamonds). (D) *a-SMA* transcripts in lung tissue from hIL-8 transgenic (n=27, black bars) and wild-type mice (n=13, white bars) were compared by rtPCR [mice aged 11-30 weeks]. (E) Flow cytometry was used to determine the kinetics and magnitude of calcium flux in response to stimulant in airway smooth muscle cells derived from 8 week old hIL-8 transgenic (n=5, black squares) and wild-type (n=4, black circles) lung tissue. (F) Immunohistochemical staining of smooth muscle actin in paraffin embedded lung sections of 12-15 week old hIL-8 transgenic (n=9) and wild-type (n=6) mice was used to quantify the average thickness of smooth muscle actin around bronchi. Representative images are shown (x20 magnification). (G) Average luminal area of bronchi were calculated. Relative expression levels of transcripts for the epithelial mesenchymal transition related proteins (H) E-cadherin (I) occludin, (J) vimentin and (K) fibronectin were compared in lung tissue from hIL-8 transgenic and wild-type mice at (i) 10 weeks, (ii) 20 weeks and (iii) 27 weeks of age (n=5 per group). Error bars represent mean±SEM. Statistical significance was determined using an unpaired t-test (*$p<0.05$, **$p<0.005$, ***$p<0.0005$).

Figure 7. Chronic exposure to hIL-8 in the lung results in altered expression of tight junction associated proteins, damage to the bronchial epithelium and functionally leaky tight junctions. (A) A schematic diagram of key tight junction

Copyright © 2018 by the American Thoracic Society

AJRCMB Articles in Press. Published on 12-June-2018 as 10.1165/rcmb.2018-0007OC

associated proteins is shown. Relative expression levels of transcripts for the tight junction proteins (B) Claudin 18, (C) JAM1 and (D) ZO-1 were compared in lung tissue from hIL-8 transgenic (black bars) and wild-type mice (white bars) at (i) 10 weeks, (ii) 20 weeks and (iii) 27 weeks of age (n = 5 per group). (E) Representative immunofluorescence staining for DAPI (Blue), Claudin 18 (Green) and hIL8 (red) in frozen lung and small intestine tissue sections of 26-27 week old hIL-8 transgenic (n=6) and wild-type mice (n=6) is shown. (F) Images were scored by 4 blinded individuals using a pre-defined scale to assess epithelial damage. Data are shown as (i) average scores for hIL-8 transgenic and wild-type groups and (ii) as the percentage of images per group assigned a score of 0-1 (striped bars) or 2-3 (light grey bars). (G) Concentration of albumin in the BAL fluid from hIL-8 transgenic (black squares) (n=14) and wild-type mice (black circles) (n=6) at 10-15 weeks of age was determined by ELISA. Error bars represent mean ± SEM. Statistical significance was determined using an unpaired t-test (*$p<0.05$, **$p<0.005$, ***$p<0.0005$).

Copyright © 2018 by the American Thoracic Society

REFERENCES

1. Yoshimura T, Matsushima K, Tanaka S, Robinson EA, Appella E, Oppenheim JJ, Leonard EJ. Purification of a human monocyte-derived neutrophil chemotactic factor that has peptide sequence similarity to other host defense cytokines. *Proc. Natl. Acad. Sci. USA* 1987;84:9233-9237.

2. Schroder JM, Mrowietz U, Morita E, Christophers E. Purification and partial biochemical characterization of a human monocyte-derived, neutrophil-activating peptide that lacks interleukin 1 activity. *J Immunol* 1987;139:3474-3483.

3. Auer PL, Teumer A, Schick U, O'Shaughnessy A, Lo KS, Chaml N, Carlson C, de Denus S, Dube M, Haessler J, Jackson RD, Kooperberg C, Lemleux Perreault L, Nauck M, Peters U, Rloux JD, Schmldt F, Turcot V, Volker U, Volzke H, Grelnacher A, Hsu L, Tardlf J, Diaz GA, Relner AP, Lettre G. Rare and low-frequency coding variants in CXCR2 and other genes are associated haematological traits. *Nat Genet* 2014;46:629-634.

4. McGarvey LP, Dunbar D, Martin SL, Brown V, Macmahon J, Ennis M, Elborn JS. Cytokine concentrations and neutrophil elastase activity in bronchoalveolar lavage and induced sputum from patients with cystic fibrosis, mild asthma and healthy volunteers. *J Cyst Fibros* 2002;1:269-275.

Copyright © 2018 by the American Thoracic Society

AJRCMB Articles in Press. Published on 12-June-2018 as 10.1165/rcmb.2018-0007OC

5. Yamamoto C, Yoneda T, Yoshikawa M, Fu A, Tokuyama T, Tsukaguchi K, Narita N. Airway inflammation in COPD assessed by sputum levels of interleukin-8. *Chest* 1997;112:505-510.

6. Car BD, Meloni F, Luisetti M, Semenzato G, Gialdroni-Grassi G, Walz A. Elevated IL-8 and MCP-1 in the bronchoalveolar lavage fluid of patients with idiopathic pulmonary fibrosis and pulmonary sarcoidosis. *Am J Respir Crit Care Med* 1994;149:655-659.

7. Aggarwal A, Baker CS, Evans TW, Haslam PL. G-CSF and IL-8 but not GM-CSF correlate with severity of pulmonary neutrophilia in acute respiratory distress syndrome. *Eur Respir J* 2000;15:895-901.

8. Gibson PG, Simpson JL, Saltos N. Heterogeneity of airway inflammation in persistent asthma: evidence of neutrophilic inflammation and increased sputum interleukin-8. *Chest* 2001;119:1329-1336.

9. Ahn M, Park B, Lee S, Park S, Park J, Kim D, Jang A, Park J, Shin H, Uh S, Kim Y, Kim Y, Han S, Jung K, Lee K, Jeong S, Park J, Choi B, Park I, Chung M, Shin H, Song J, Kim D, Park C, Shim Y. A promoter SNP rs4073T>A in the common allele of the interleukin 8 gene is associated with the development of idiopathic pulmonary fibrosis via the IL-8 protein enhancing mode. *Resp Res* 2011;12:73

Copyright © 2018 by the American Thoracic Society

10. Hillian AD, Londono D, Dunn JM, Goddard KA, Pace RG, Knowles MR, Drumm ML. Modulation of cystic fibrosis lung disease by variants in interleukin-8. *Genes Immun* 2008;9:501-508.

11. Matheson MC, Ellis JA, Raven J, Hayden Walters E, Abramson MJ. Association of IL8, CXCR2 and TNF-α polymorphisms and airway disease. *J Hum Genet* 2006;51:196-203.

12. Behndig AF, Mudway IS, Brown JL, Stenfors N, Helleday R, Duggan ST, Wilson SJ, Boman C, Cassee FR, Frew AJ, Kelly FJ, Sandström T, Blomberg A. Airway antioxidant and inflammatory responses to diesel exhaust exposure in healthy humans. *Eur Respir J.* 2006; 27:359-65.

13. Simpson JL, Phipps S, Gibson PG. Inflammatory mechanisms and treatment of obstructive airway diseases with neutrophilic bronchitis. *Pharmacology and Therapeutics* 2009;124:86-95.

14. Matsushima K, Morishita K, Yoshimura T, Lavu S, Kobayashi Y, Lew W, Appella E, Kung HF, Leonard EJ, Oppenheim JJ. Molecular cloning of a human monocyte-derived neutrophil chemotactic factor (MDNCF) and the induction of MDNCF mRNA by interleukin 1 and tumor necrosis factor. *J Exp Med* 1988;167:1883-1893.

Copyright © 2018 by the American Thoracic Society

AJRCMB Articles in Press. Published on 12-June-2018 as 10.1165/rcmb.2018-0007OC

15. Lee J, Horuk R, Rice GC, Bennett GL, Camerato T, Wood WI. Characterization of two high affinity human interleukin-8 receptors. *J Biol Chem* 1992;267:16283-16287.

16. Morohashi H, Miyawaki T, Nomura H, Kuno K, Murakami S, Matsushima K, Mukaida N. Expression of both types of human interleukin-8 receptors on mature neutrophils, monocytes, and natural killer cells. *J Leukoc Biol* 1995;57:180-187.

17. Govindaraju V, Michoud MC, Al-Chalabi M, Ferraro P, Powell WS, Martin JG. Interleukin-8: novel roles in human airway smooth muscle cell contraction and migration. *Am J Physiol Cell Physiol* 2006;291:C957-965.

18. Heidemann J, Ogawa H, Dwinell MB, Rafiee P, Maaser C, Gockel HR, Otterson MF, Ota DM, Lugering N, Domschke W, Binion DG. Angiogenic effects of interleukin 8 (CXCL8) in human intestinal microvascular endothelial cells are mediated by CXCR2. *J Biol Chem* 2003;278:8508-8515.

19. Walz A, Peveri P, Aschauer H, Baggiolini M. Purification and amino acid sequencing of NAF, a novel neutrophil-activating factor produced by monocytes. *Biochem Biophys Res* Commun 1987;149:755-761.

Copyright © 2018 by the American Thoracic Society

20. Takeda N, Sumi Y, Prefontaine D, Al-Abri J, Al-Heialy N, Al-Ramli W, Michoud MC, Martin JG, Hamid Q. Epithelium-derived chemokines induce airway smooth muscle cell migration. *Clin Exp Allergy* 2009;39:1018-1026.

21. Russo RC, Guabiraba R, Garcia CC, Barcelos LS, Roffe E, Souza AL, Amaral FA, Cisalpino D, Cassali GD, Doni A, Bertini R, Teixeira MM. Role of the chemokine receptor CXCR2 in bleomycin-induced pulmonary inflammation and fibrosis. *Am J Respir Cell Mol Biol* 2009;40:410-421.

22. Herbold W, Maus R, Hahn I, Ding N, Srivastava M, Christman JW, Mack M, Reutershan J, Briles DE, Paton JC, Winter C, Welte T, Maus UA. Importance of CXC chemokine receptor 2 in alveolar neutrophil and exudate macrophage recruitment in response to pneumococcal lung infection. *Infect Immun* 2010;78:2620-2630.

23. De Soyza A, Pavord I, Elborn JS, Smith D, Wray H, Puu M, Larsson B, Stockley R. A randomised, placebo-controlled study of the CXCR2 antagonist AZD5069 in bronchiectasis. *Eur Respir J* 2015;46:1021-1032.

24. Bozic CR, Gerard NP, von Uexkull-Guldenband C, Kolakowski LF, Conklyn MJ, Breslow R, Showell HJ, Gerard C. The murine interleukin 8 type B receptor homologue and its ligands. *J Biol Chem* 1994;269:29355-29358.

Copyright © 2018 by the American Thoracic Society

AJRCMB Articles in Press. Published on 12-June-2018 as 10.1165/rcmb.2018-0007OC

25. Rot A. Chemotactic potency of recombinant human neutrophil attractant/activation protein-1 (Interleukin-8) for polymorphonuclear leukocytes of different species. *Cytokine* 1991;3:21-27.

26. Singer M, Sansonetti PJ. IL-8 is a key chemokine regulating neutrophil recruitment in a new mouse model of *Shigella*-Induced Colitis. *J Immunol* 2004;173:4197-4206.

27. Clifford RJ, Milillo M, Prestwood J, Quintero R, Zurawski DV, Kwak YI, Waterman PE, Lesho EP, Mc Gann P. Detection of bacterial 16S rRNA and identification of four clinically important bacteria by real-time PCR. *PLoS One* 2012;7:e48558.

28. Kishimoto TK, Jutila MA, Berg EL, Butcher EC. Neutrophil Mac-1 and MEL-14 adhesion proteins inversely regulated by chemotactic factors. *Science* 1989;245:1238-1241.

29. Weiss SJ, Young J, LoBuglio AF, Slivka A, Nimeh NF. Role of hydrogen peroxide in neutrophil-mediated destruction of cultured endothelial cells. *J Clin Invest* 1981;68:714-721.

30. Feniger-Barish R, Ran M, Zaslaver A, Ben-Baruch A. Differential modes of regulation of cxc chemokine-induced internalization and recycling of human CXCR1 and CXCR2. *Cytokine* 1999;11:996-1009.

Copyright © 2018 by the American Thoracic Society

31. Koch MA, Thomas KR, Perdue NR, Smigiel KS, Srivastava S, Campbell DJ. T-bet(+) Treg cells undergo abortive Th1 cell differentiation due to impaired expression of IL-12 receptor β2. *Immunity* 2012 21;37:501-10.

32. Levine AG, Medoza A, Hemmers S, Moltedo B, Niec RE, Schizas M, Hoyos BE, Putintseva EV, Chaudhry A, Dikiy S, Fujisawa S, Chudakov DM, Treuting PM, Rudensky AY. Stability and function of regulatory T cells expressing the transcription factor T-bet. *Nature* 2017 15;546:421-425.

33. Kirkham S, Sheehan JK, Knight D, Richardson PS, Thornton DJ. Heterogeneity of airways mucus: variations in the amounts and glycoforms of the major oligomeric mucins MUC5AC and MUC5B. *Biochem J* 2002;361:537-546.

34. Voynow JA, Gendler SJ, Rose MC. Regulation of mucin genes in chronic inflammatory airway diseases. *Am J Respir Cell Mol Biol* 2006;34:661-665.

35. Lambert RK, Wiggs BR, Kuwano K, Hogg JC, Pare PD. Functional significance of increased airway smooth muscle in asthma and COPD. *J Appl Physiol* 1985;74:2771-2781.

Copyright © 2018 by the American Thoracic Society

AJRCMB Articles in Press. Published on 12-June-2018 as 10.1165/rcmb.2018-0007OC

36. Kalluri R, Weinberg RA. The basics of epithelial-mesenchymal transition. *J Clin Invest* 2009;119;1420-1428.

37. Milara J, Perio T, Serrano A, Cortijo J. Epithelial to mesenchymal transition is increased in patients with COPD and induced by cigarette smoke. *Thorax* 2013;68:410-420.

38. Coyne CB, Vanhook MK, Gambling TM, Carson JL, Boucher RC, Johnson LG. Regulation of airway tight junctions by proinflammatory cytokines. *Mol Biol Cell* 2002;13:3218-3234.

39. Koval M, Ward C, Findley MK, Rose-Page S, Helms MN, Roman J. Extracellular matrix influences alveolar claudin expression and barrier function. *Am J Respir Cell Mol Biol* 2010;42:172-180.

40. Wray C, Mao Y, Pan J, Chandrasena A, Piasta F, Frank JA. Claudin-4 augments alveolar epithelial barrier function and is induced in acute lung injury. *Am J Physiol Lung Cell Mol Physiol* 2009 297:L219-27.

41. Endeman H, Meijvis SC, Rijkers GT, van Velzen-Blad H, van Moorsel CH, Grutters JC, Biesma DH. Systemic cytokine response in patients with community-acquired pneumonia. *Eur Respir J* 2011;37:1431-1438.

Copyright © 2018 by the American Thoracic Society

42. Tsai WC, Strieter RM, Wilkowski JM, Bucknell KA, Burdick MD, Lira SA, Standiford TJ. Lung-specific transgenic expression of KC enhances resistance to Klebsiella pneumoniae in mice. *J Immunol* 1998;161:2435-2440.

43. Asfaha S, Dubeykovskiy AN, Tomita H, Yang X, Stokes S, Shibata W, Freidman RA, Ariyama H, Dubeykovskaya ZA, Muthupalani S, Ericksen R, Frucht H, Fox JG, Wang TC. Mice the express human interleukin-8 have increased mobilization of immature myeloid cells, which exacerbates inflammation and accelerates colon carcinogenesis. *Gastroenterology* 2013;144:155-166.

44. Cromwell O, Hamid Q, Corrigan CJ, Barkans J, Meng Q, Collins PD, Kay AB. Expression and generation of interleukin-8, IL-6 and granulocyte-macrophage colony-stimulating factor by bronchial epithelial cells and enhancement by IL-1 beta and tumor necrosis factor-alpha. *Immunology* 1992;77:330-337.

45. Soler N, Ewig S, Torres A, Filella X, Gonzalez J, Zaubet A. Airway inflammation and bronchial microbial patterns in patients with stable chronic obstructive pulmonary disease. *Eur Respir J* 1999;14:1015-1022.

46. Hollander C, Sitkauskiene B, Sakalauskas R, Westin U, Janciauskiene SM. Serum and bronchial lavage fluid concentrations of IL-8, SLP1, sCD14 and sICAM-1 in patients with COPD and asthma. *Respiratory Medicine* 2007;101:1947-1963.

Copyright © 2018 by the American Thoracic Society

AJRCMB Articles in Press. Published on 12-June-2018 as 10.1165/rcmb.2018-0007OC

47. Koh AY, Priebe GP, Ray C, Van Rooijen N, Pier GB. Inescapable need for neutrophils as mediators of cellular innate immunity to acute *Pseudomonas aeruginosa* Pneumonia. *Infect and Immun* 2009;77:5300-5310.

48. Lovewell RR, Patankar YR, Berwin B. Mechanisms of phagocytosis and host clearance of *Pseudomonas aeruginosa*. *Am J Physiol Lung Cell Mol Physiol* 2014;306:L591-L603.

49. Patankar YR, Mabaera R, Berwin B. Differential ASC requirements reveal a key role for neutrophils and a noncanonical IL-1β response to *Pseudomonas aeruginosa*. *Am J Physiol Lung Cell Mol Physiol* 2015;309:L902-L913.

50. Borthwick LA. The IL-1 cytokine family and its role in inflammation and fibrosis in the lung. Semin Immunopathol. 2016;38(4):517-34.

51. Ethuin F, Gerard B, Benna JE, Boutten A, Gougereot-Pocidalo MA, Jacob L, Chollet-Martin S. Human neutrophils produce interferon gamma upon stimulation by interleukin-12. *Lab Invest* 2004;84:1363-1371.

52. Charmoy M, Brunner-Agten S, Aebischer D, Auderset F, Launois P, Milon G, Proudfoot AE, Tacchini-Cottier F. Neutrophil-derived CCL3 is essential for the

Copyright © 2018 by the American Thoracic Society

rapid recruitment of dendritic cells to the site of *Leishmania major* inoculation in resistant mice. *PLoS Pathogens* 2010;6:e1000755.

53. Sandilands GP, Ahmed Z, Perry N, Davison M, Lupton A, Young B. Cross-linking of neutrophil CD11b results in rapid cell surface expression of molecules required for antigen presentation and T-cell activation. *Immunology* 2005;114:354-368.

54. Gregory LG, Mathie SA, Walker SA, Pegorier S, Jones CP, Lloyd CM. Overexpression of Smad2 drives house dust mite-mediated airway remodeling and airway hyperresponsiveness via activin and IL-25. *Am J Respir Crit Care Med*. 2010;182:143-54.

55. Campbell JD, Buckland KF, McMillan SJ, Kearley J, Oldfield WL, Stern LJ, Grönlund H, van Hage M, Reynolds CJ, Boyton RJ, Cobbold SP, Kay AB, Altmann DM, Lloyd CM, Larché M. Peptide immunotherapy in allergic asthma generates IL-10-dependent immunological tolerance associated with linked epitope suppression. *J Exp Med*. 2009;206:1535-47.

56. Martin TR, Gerard NP, Galli SJ, Drazen JM. Pulmonary responses to bronchoconstrictor agonists in the mouse. J Appl Physiol 1988; 64:2318-23.

Copyright © 2018 by the American Thoracic Society

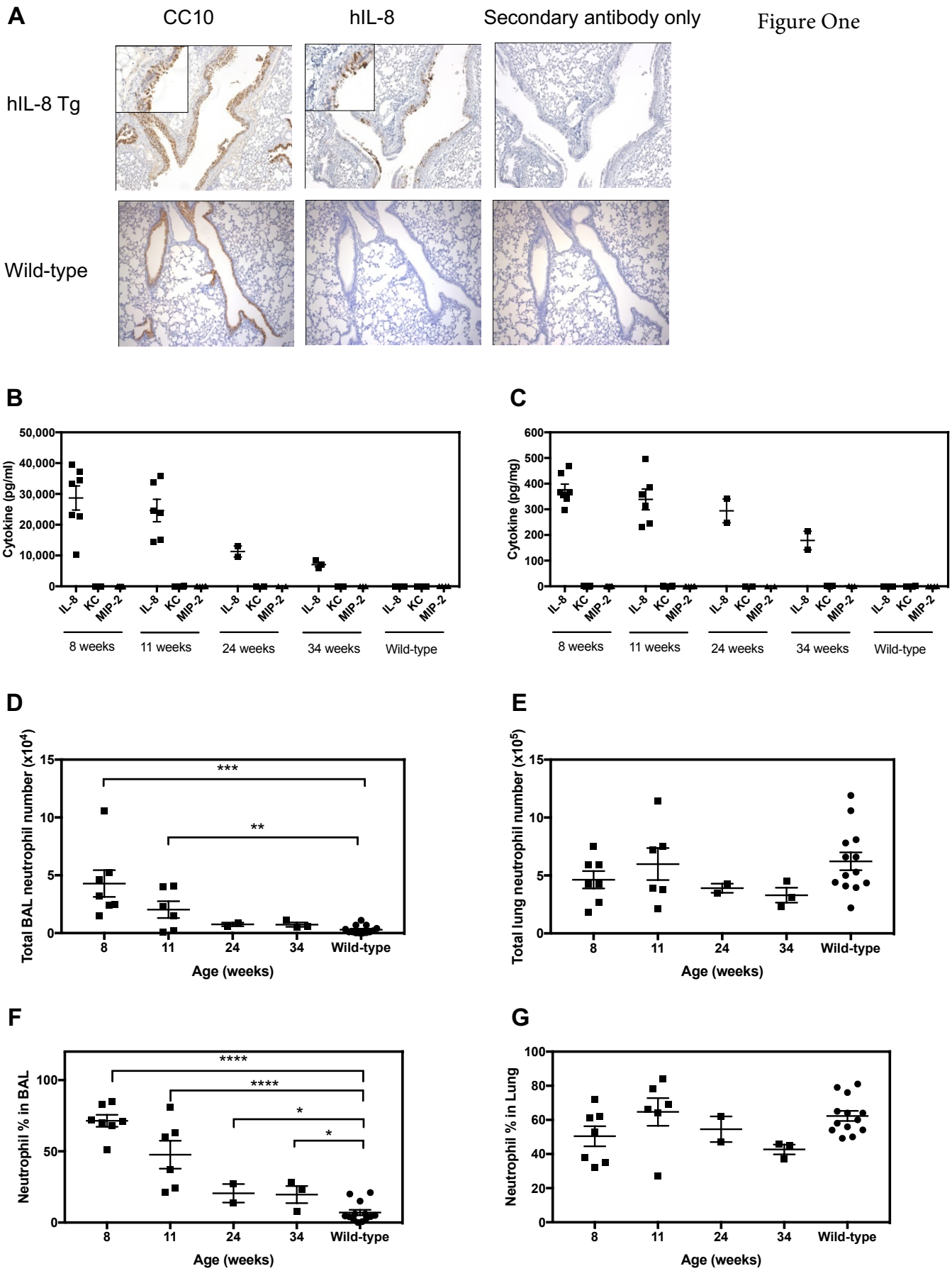
AJRCMB Articles in Press. Published on 12-June-2018 as 10.1165/rcmb.2018-0007OC

57. Hamelmann E, Schwarze J, Takeda K, Oshiba A, Larsen GL, Irvin CG, Gelfand EW. Noninvasive measurement of airway responsiveness in allergic mice using barometric plethysmography. *Am J Respir Crit Care Med.* 1997; 156:766-75.

58. Naura AS, et al. High-fat diet induces lung remodeling in ApoE-deficient mice: an association with an increase in circulatory and lung inflammatory factors. *Lab Invest*. 2009;89:1243-51

Copyright © 2018 by the American Thoracic Society

Figure One



Copyright © 2018 by the American Thoracic Society

AJRCMB Articles in Press. Published on 12-June-2018 as 10.1165/rcmb.2018-0007OC

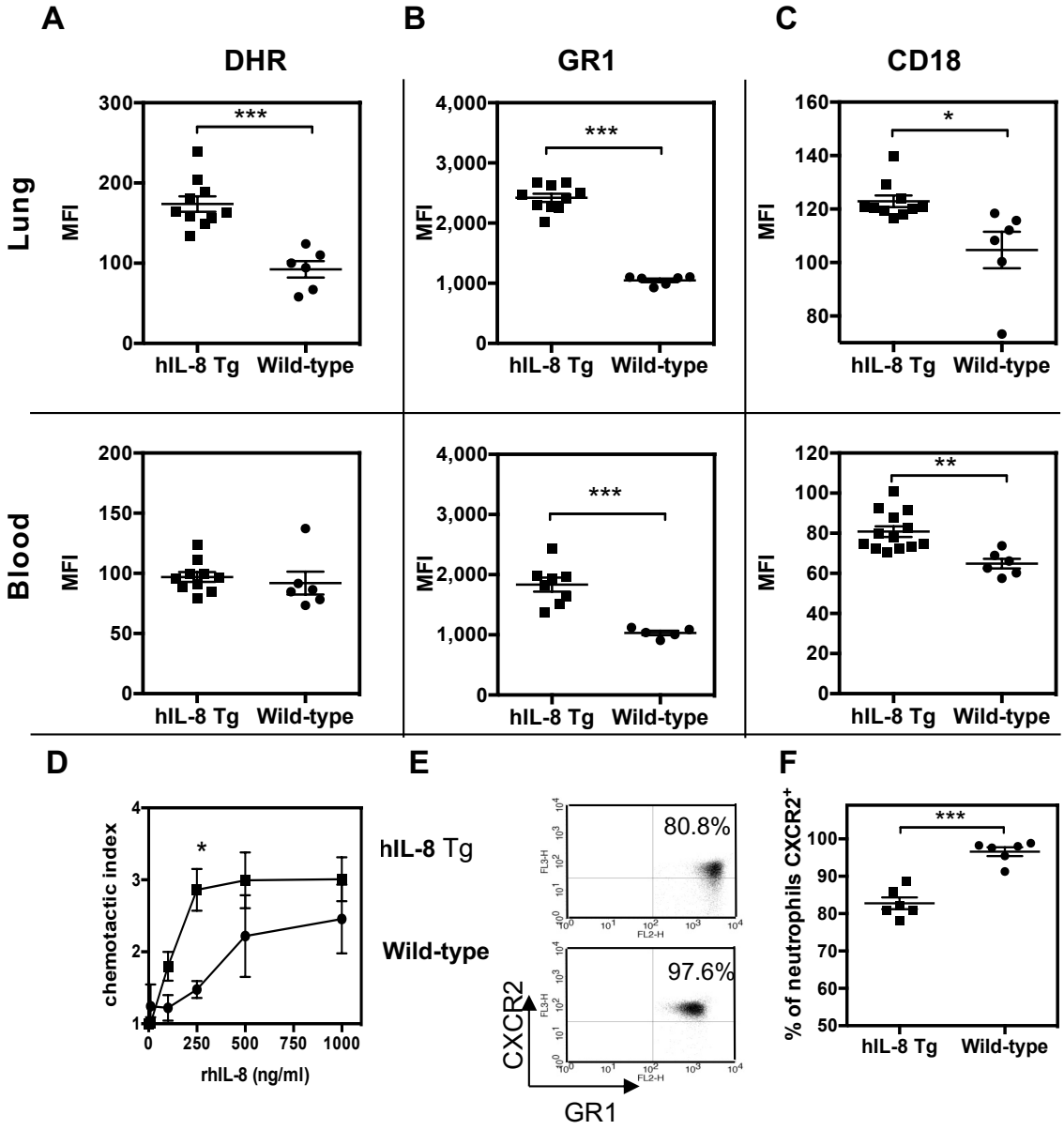


Figure 2

Copyright © 2018 by the American Thoracic Society

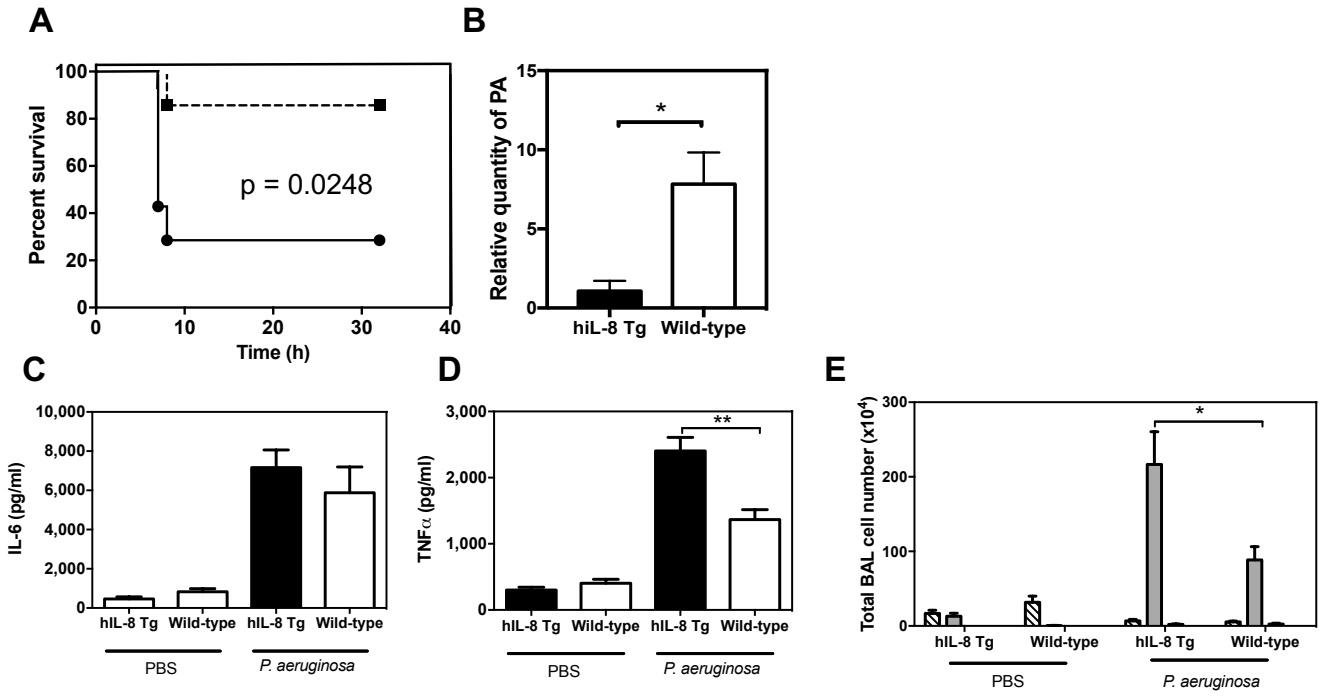
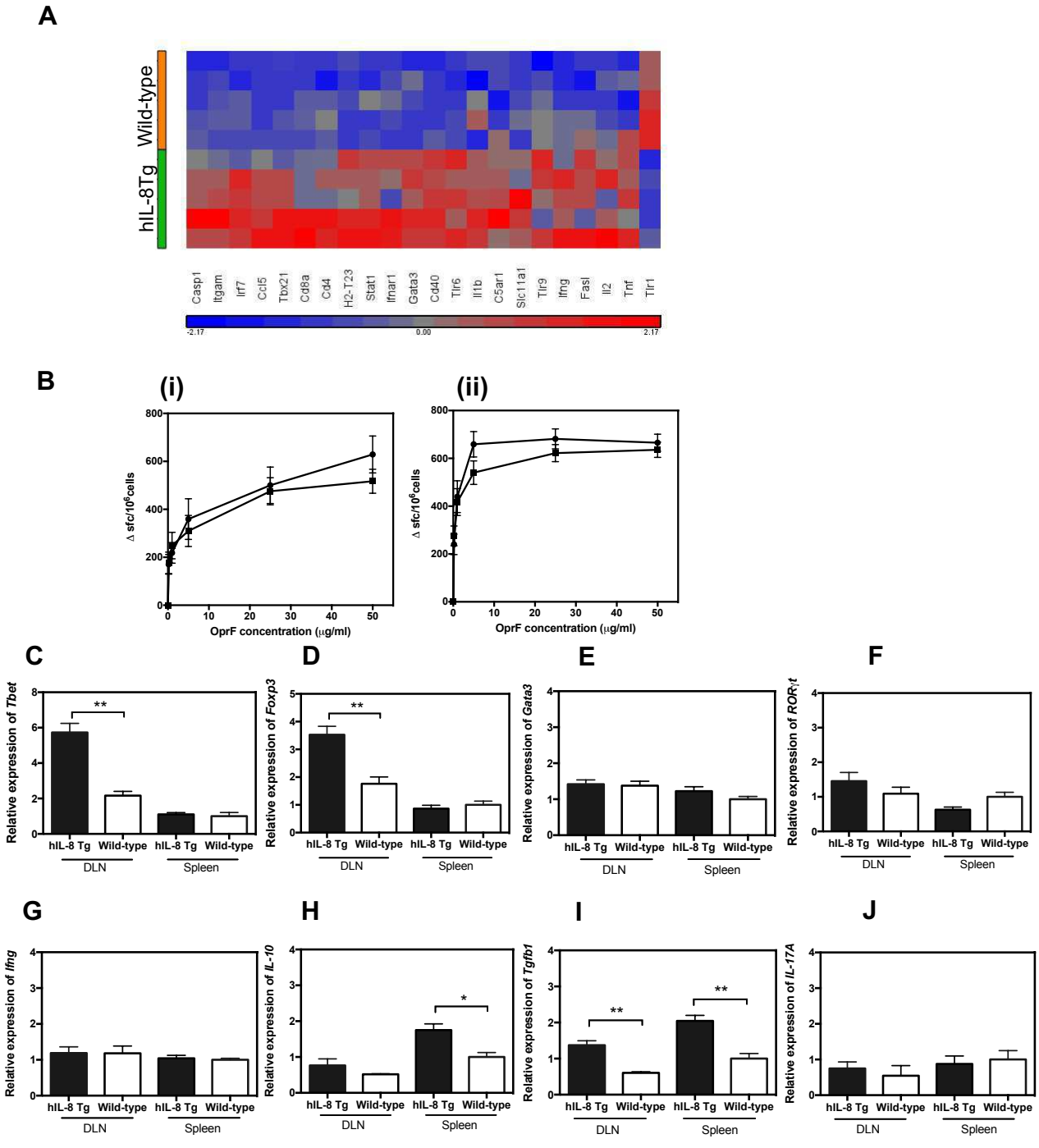


Figure 3

Copyright © 2018 by the American Thoracic Society

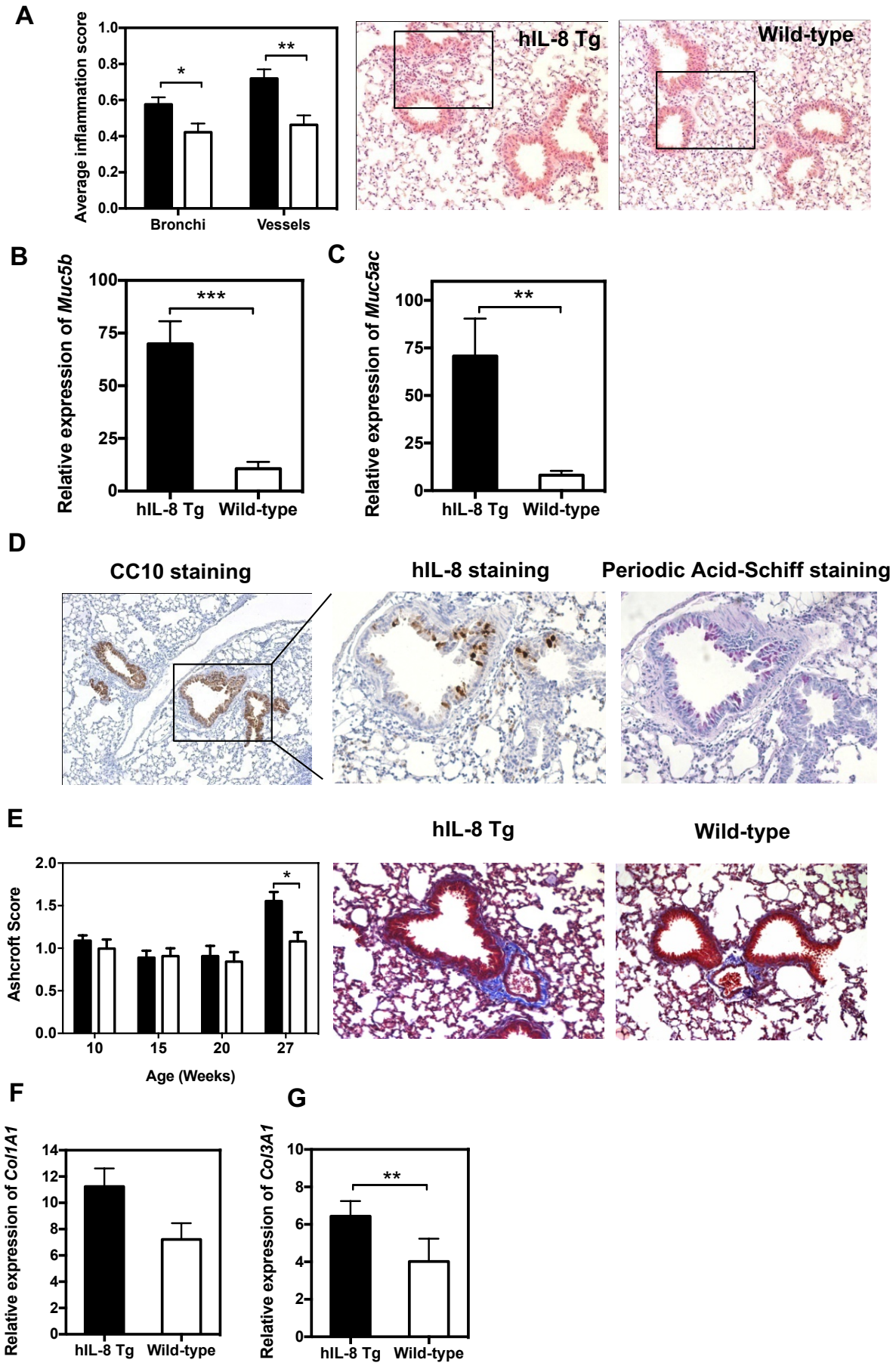
AJRCMB Articles in Press. Published on 12-June-2018 as 10.1165/rcmb.2018-0007OC

Figure 4



Copyright © 2018 by the American Thoracic Society

Figure 5



Copyright © 2018 by the American Thoracic Society

AJRCMB Articles in Press. Published on 12-June-2018 as 10.1165/rcmb.2018-0007OC

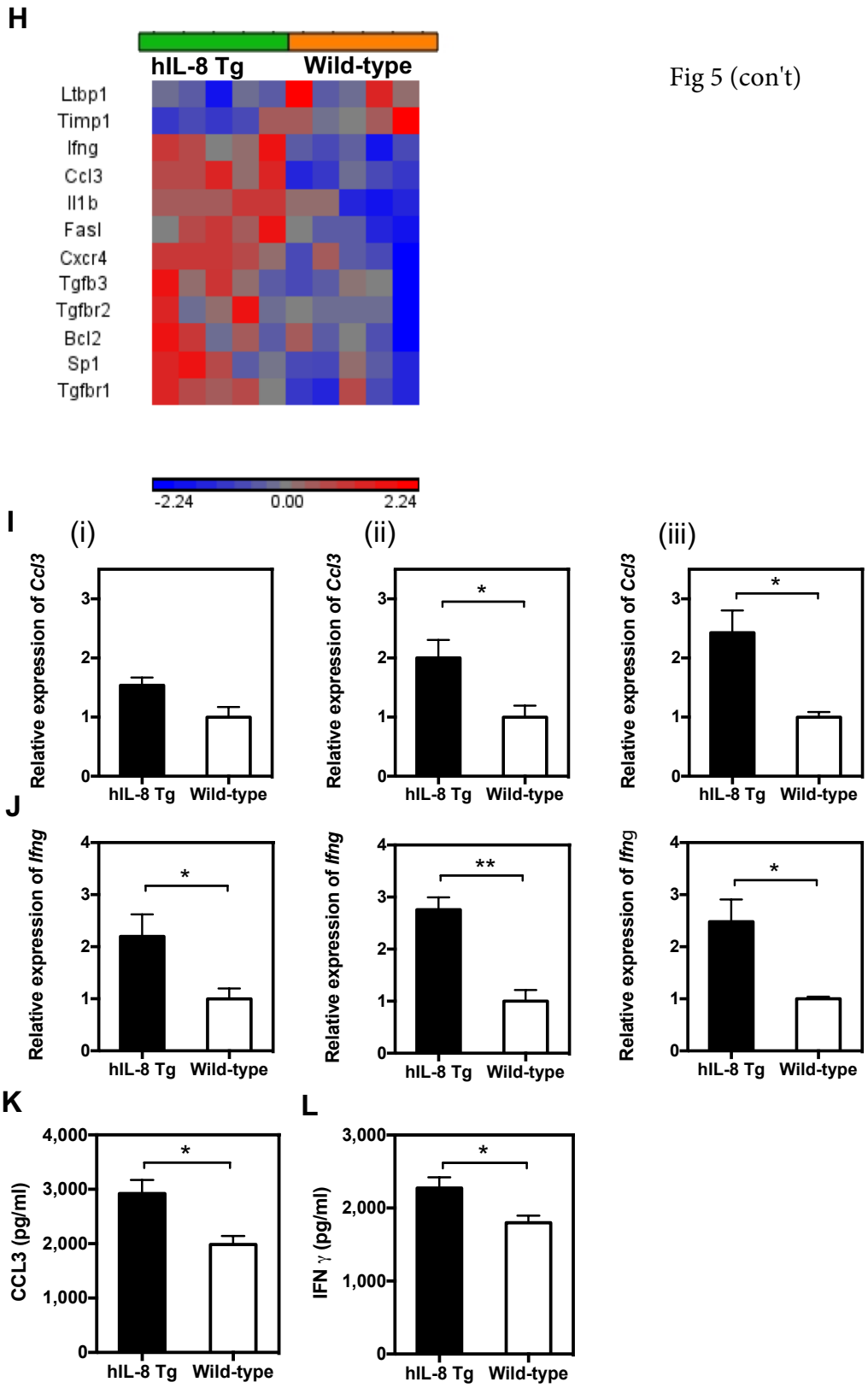


Fig 5 (con't)

Copyright © 2018 by the American Thoracic Society

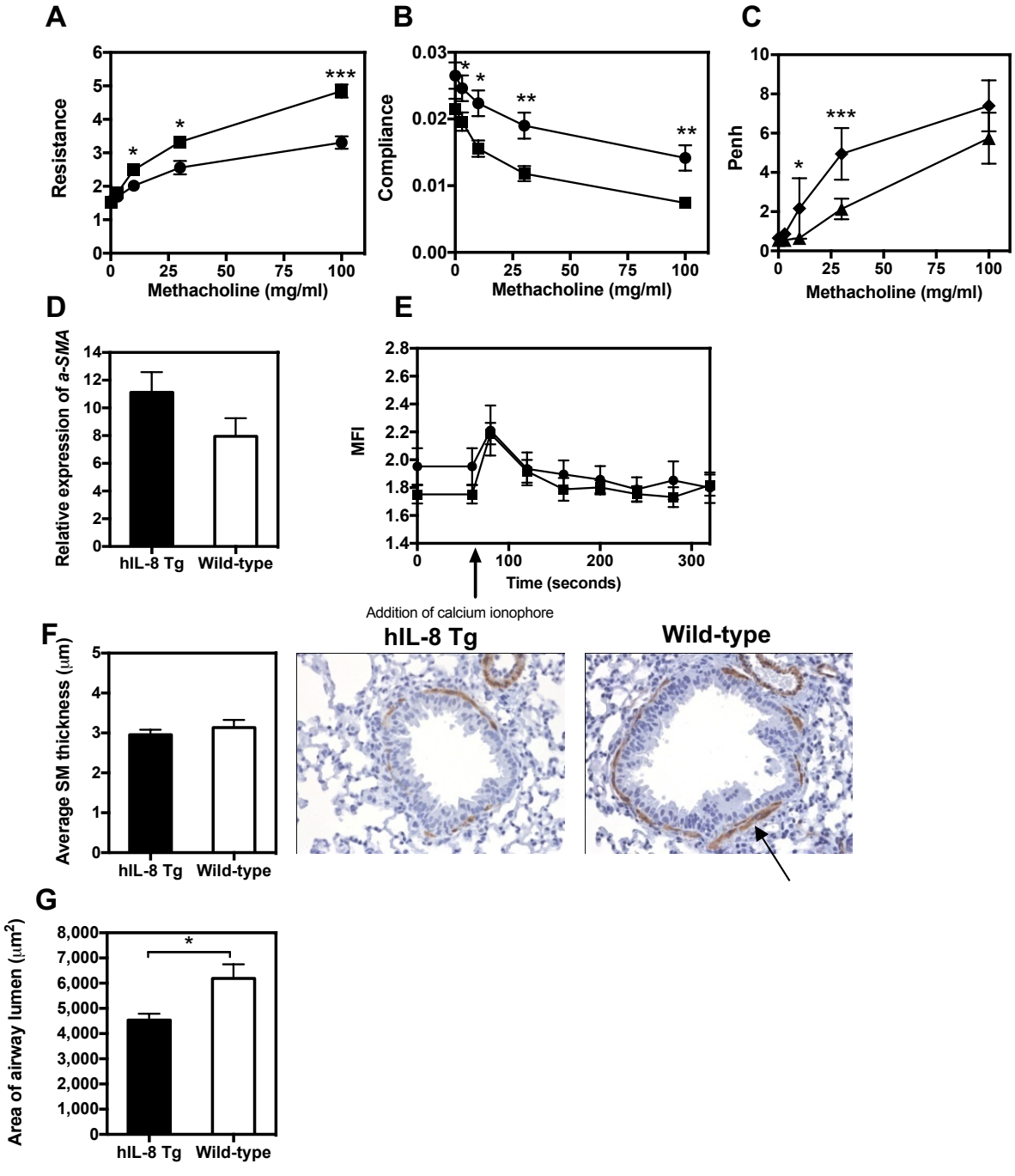


Figure 6

Copyright © 2018 by the American Thoracic Society

AJRCMB Articles in Press. Published on 12-June-2018 as 10.1165/rcmb.2018-0007OC

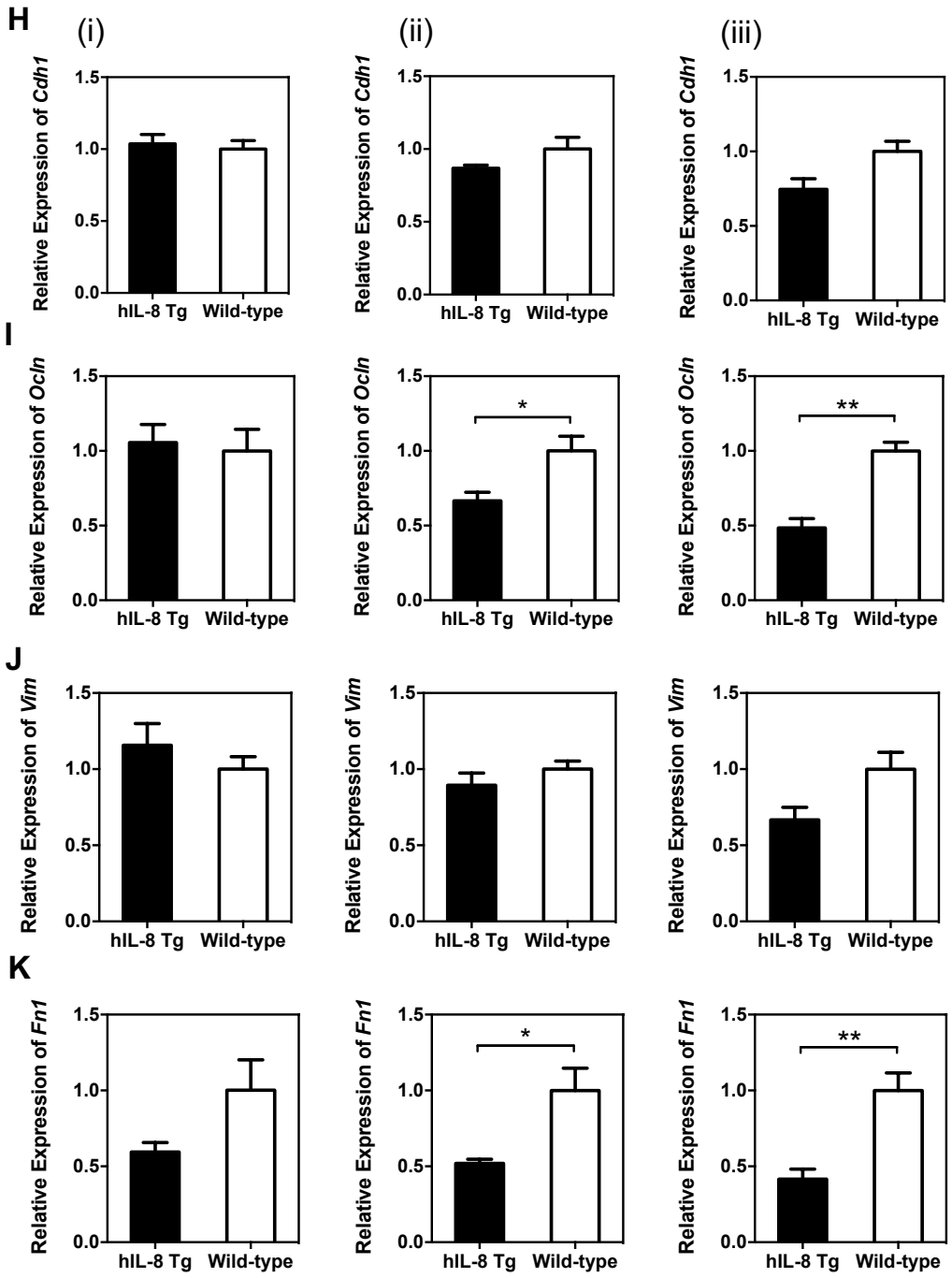


Figure 6 (con't)

Copyright © 2018 by the American Thoracic Society

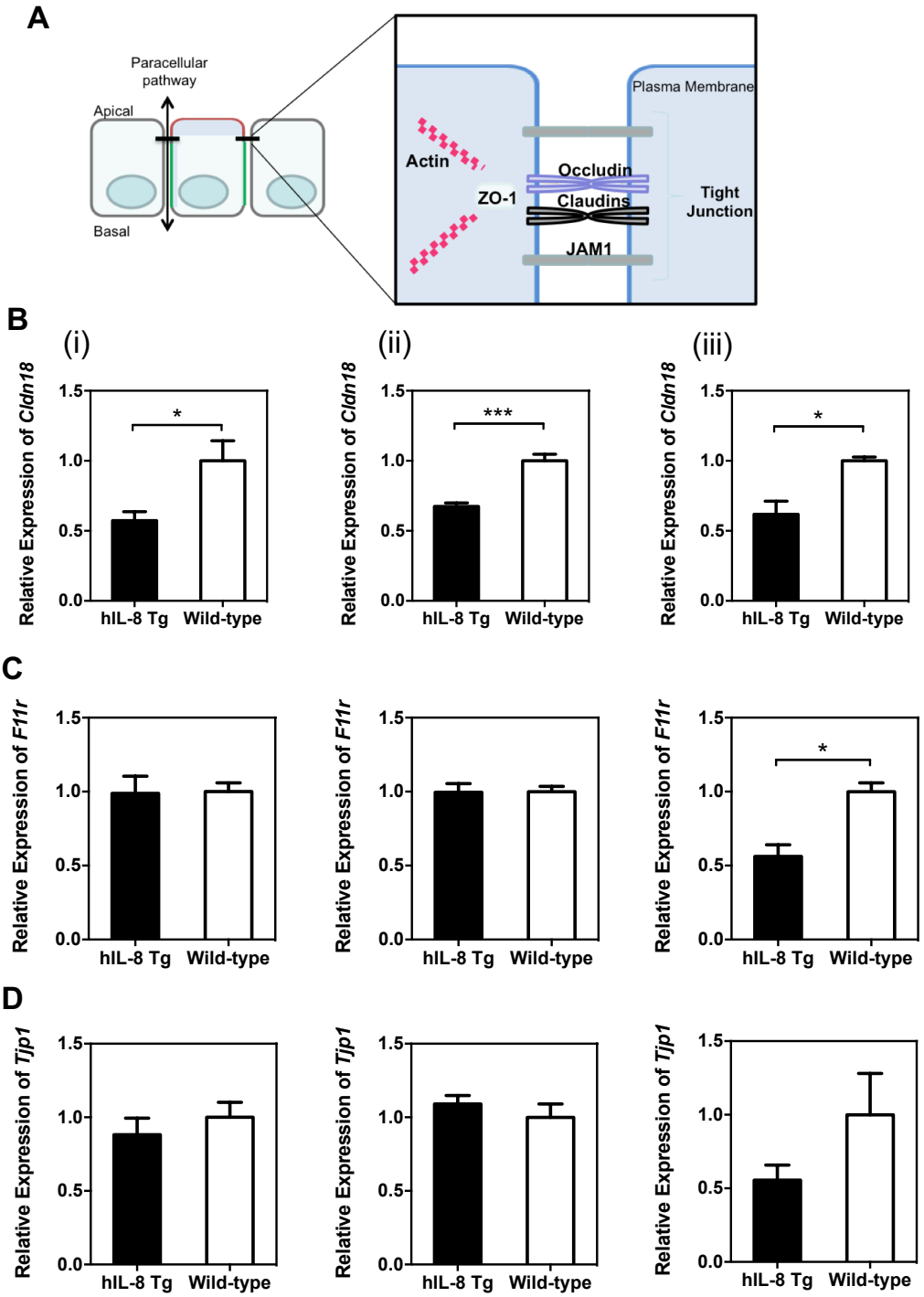
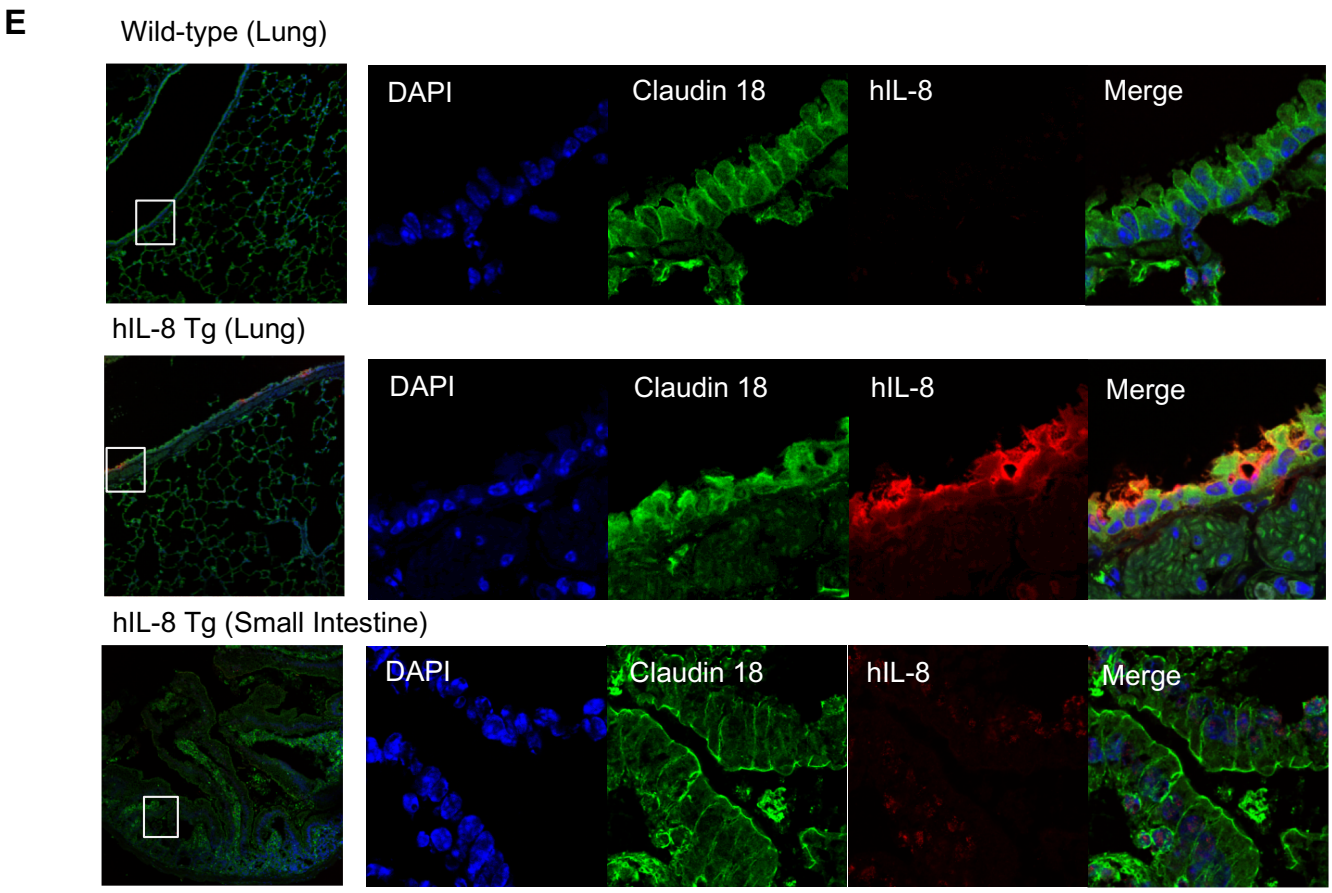


Figure 7

Copyright © 2018 by the American Thoracic Society

AJRCMB Articles in Press. Published on 12-June-2018 as 10.1165/rcmb.2018-0007OC



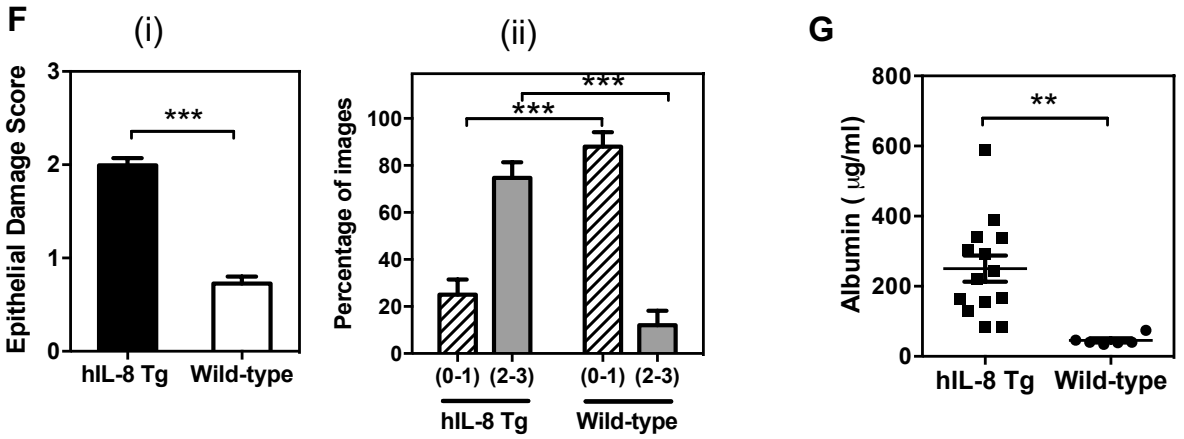


Fig 7 (con't)

Copyright © 2018 by the American Thoracic Society

AJRCMB Articles in Press. Published on 12-June-2018 as 10.1165/rcmb.2018-0007OC

LUNG DEFENSE THROUGH INTERLEUKIN-8 CARRIES A COST OF CHRONIC LUNG REMODELING AND IMPAIRED FUNCTION

Catherine J Reynolds[1,2 †], Kathryn Quigley[1,2 †], Xiaoming Cheng[1], Apurva Suresh[1], Sundas Tahir[1], Fiyyaz Ahmed-Jushuf[1], Khizr Nawab[1], Katherine Choy[2], Simone Alexandra Walker[2], Sara A Mathie[2], Malcolm Sim[1], Janet Stowell[1], Jiten Manji[1], Tracey Pollard[1], Daniel M Altmann[1], Rosemary J Boyton[1,2,3*]

[1]Lung Immunology Group, Infectious Disease and Immunity, Department of Medicine, Imperial College London, W12 ONN UK

[2]MRC & Asthma UK Centre in Allergic Mechanisms of Asthma, UK

[3]Department of Respiratory Medicine, Royal Brompton and Harefield NHS Foundation Trust, SW3 6NP UK

SUPPLEMENTAL EXPERIMENTAL METHODS

Mice

To generate hIL-8 transgenic mice the coding sequence of hIL-8 was amplified from human PBMC cDNA by PCR (FP 5'- AGGAATTCTGTAAACATGACTTCCAAGC, RP 5'- GCGAATTCTTATGAGTTCTCAGCCCTCTTC) and subcloned into a pBluescript II vector downstream of the CC10 promoter (supplied by J. Whitsett, University of Cincinnati, USA) and upstream of a rabbit β-globin poly (A) sequence (supplied by Helen Bodmer, UK) (Supplementary figure 1A). The construct was linearized and bacterial sequences removed by XhoI (R6161, Promega, USA) restriction digest prior to pro-nuclear microinjection into fertilized FVBN oocytes. Founders were

Copyright © 2018 by the American Thoracic Society

AJRCMB Articles in Press. Published on 12-June-2018 as 10.1165/rcmb.2018-0007OC

identified by PCR and Southern and the transgenic line established by crossing the founder animal with C57BL/6 mice and backcrossing for at least 4 generations. Wild-type animals were either transgene negative littermates or age and sex matched C57BL/6 mice. Mouse experiments were performed within U.K. Home Office legislation under the terms of the Project License PPL 70/7708 granted for this work under the "Animals (Scientific Procedures) Act 1986.

RT-PCR and real time PCR analysis

RNA was extracted from homogenized tissue samples using TRIzol ® (15596026, ThermoFisher Scientific, USA). cDNA was reverse transcribed using SuperScript III (18080093, ThermoFisher Scientific, USA). hIL-8 cDNA transcripts were detected using a multiplex PCR containing primers specific for hIL-8 (see above) and 18s (AM1716, ThermoFisher Scientific, USA). Real time PCR reactions were performed using Brilliant II QPCR Low Rox Master Mix (600806, Agilent, USA) and the appropriate concentrations of gene specific primers and probe. *Gapdh (Mm99999915_g1)*, *KC (Mm04207460_m1)*, *MIP-2 (Mm00436450_m1)*, *Tbx21(Mm00450960_m1), Foxp3 (Mm00475162_m1), Gata3 (Mm00484683_m1), RORγt (Mm01261022_m1), Ifng (Mm01168134_m1), Il10 (Mm01288386_m1), Tgfb1 (Mm01178820_m1), Il17a (Mm00439618_m1), Ccl3 (Mm00441259_g1), Cldn18 (Mm00517321_m1), F11r (Mm00554113_m1)*, *Tjp1 (Mm00493699_m1)*, *Ocln (Mm00500912_m1)*, *Cdh1 (Mm01247357_m1), Fn1 (Mm01256744_m1),* and *Vim* (Mm01333430_m1) primers and probes were purchased from Applied Biosystems (Assays-on-Demand™ Gene expression assays, Applied Biosystems, USA).

Copyright © 2018 by the American Thoracic Society

Muc5b

(FP 5'- GCACGTAAATGCGACTGTCT, RP 5'- ATGGACCTTGCTCTCCTGAC,

Probe 5'- [6FAM]TATCCAAGTACTCCATGGAGGCCC[TAM]),

Muc5ac

(FP 5'- TCCCTTACCTAACCAGCAGAA, RP 5'- GGGAGTACATGGAGATGCTGT,

Probe 5'- [6FAM]GAGGGCCCAGTGAGCATCTCCTACT[TAM]),

Col1A1

(FP 5'- TAAGGGTACCGCTGGAGAAC, RP 5'- GTTCACCTCTCTCACCAGCA,

Probe 5'- [6FAM]AGAGCGAGGCCTTCCCGGAC[TAM]),

Col3A1

(FP 5'- TTCTACACCTGCTCCTGTGC, RP 5'- AGACCTGGTTGTCCTGGAAG,

Probe 5'- [6FAM]TCCGGGTCCTCCTGGCATTC[TAM])

a-SMA (FP 5'- AAACGAACGCTTCCGCTG, RP 5'- GATGCCCGCTGACTCCAT,

Probe 5'- [6FAM]CCAGAGACTCTCTTCCAGCCTCTTTCATTG[TAM])

Muc5b, Muc5ac, *Col1A1, Col3A1*, and *a-SMA* primers and probes were purchased from Sigma-Aldrich UK.

PCR array

cDNA was synthesized from 700ng RNA using the RT2 First strand kit (330401, Qiagen, Germany). Each cDNA sample was run on a separate murine innate and adaptive immune response (PAMM-052Z), murine fibrosis (PAMM-120A) or murine tight junction (PAMM-143Z) RT^2 Profiler^{TM} PCR array plate (Qiagen, Germany). Plates were run on a Stratagene Mx3000p RT PCR machine and data was analysed using Partek Genomics Suite version 6.6 (Partek, USA)

Copyright © 2018 by the American Thoracic Society

AJRCMB Articles in Press. Published on 12-June-2018 as 10.1165/rcmb.2018-0007OC

Bronchoalveolar lavage and lung tissue preparation

To collect BAL fluid, mice were exsanguinated by cardiac puncture followed by cannulation of the trachea. Lungs were lavaged 3 times with 0.4ml PBS (10010056, ThermoFisher Scientific, USA) and BAL fluid pooled for each mouse. Snap frozen lung samples were prepared for ELISA analysis by homogenising at a concentration of 100 mg/ml in Hanks's balanced salt solution (14175046, ThermoFisher Scientific, USA) containing a complete mini protease inhibitor cocktail (11836153001, Roche Diagnostics GmbH, Germany). For experiments requiring lung disaggregation, tissue was finely chopped and placed into 5ml of RPMI 1640 medium (31870074, ThermoFisher Scientific, USA) containing 0.15mg/ml Collagenase D (11088858001, roche Diagnostics GmbH, Germany) and 25 μg/ml DNase I (11284932001, Roche Diagnostics GmbH, Germany). Samples were incubated with shaking for 1h at 37^{o}C before passing through a 70μm cell strainer. For differential cell counting, 5 x 10^4 BAL or lung cells were spun onto polysine glass microscope slides and fixed in methanol for 3 minutes. Slides were stained by immersing in Wright Giemsa stain (WG16, Sigma-Aldrich, USA) for 1 minute followed by distilled water for 6 minutes without agitation. A total of 300 cells were counted on each slide with cell types distinguished by size, cytoplasmic staining and nuclear morphology.

ELISA

Paired antibodies specific for hIL-8 (MAB208 and BAF208), TNFα (AF-410-NA and BAF410), CCL3 (AF-450-NA and VAF450), IFNγ (MAB785 and BAF485), KC (Duoset DY453), MIP-2 (Duoset DY452) (R&D systems, USA) and IL-6 (KMC0061, ThermoFisher Scientific, USA) were used for cytokine ELISAs. Albumin

Copyright © 2018 by the American Thoracic Society

concentrations in BAL fluid were determined using an ELISA based kit (E90-134, Bethyl Laboratories, USA)

Immunohistochemistry

Immunohistochemical staining for CC10, hIL-8 and smooth muscle actin (SMA) proteins was performed on 4 μm wax embedded lung sections that had been deparaffinised and heated in citrate buffer for epitope retrieval. Goat anti-mouse CC10 at 0.2μg/ml (sc-9773, Santa Cruz Biotechnology, USA), rabbit anti-human IL-8 at 2μg/ml (AHP781, Bio-Rad, USA) and rabbit anti-mouse SMA at 0.4μg/ml (ab5694, Abcam, UK) were used as primary antibodies in combination with appropriate biotinylated secondary antibodies and staining was visualised using the peroxidase based ABC reagent (PK-4007, Vector Laboratories, USA) followed by DAB substrate (SK-4100, Vector Laboratories, USA). Measurements of smooth muscle diameter around bronchioles and luminal area on SMA stained lung sections were done on images taken at x40 magnification (Leica DFA300FX microscope) with Leica QWin measurement software. Four images were taken per mouse and a total of 10 measurements taken per image.

Immunofluorescence staining of Claudin 18 and hIL-8 proteins was done using frozen tissue sections. Primary antibodies rabbit anti-mouse Claudin 18 at 5μg/ml (38-8000, ThermoFisher Scientific, USA) and goat anti-human IL-8 at 10μg/ml (ab10769, Abcam, UK) were used in combination with donkey anti-rabbit alexa fluor 546 (A10040, ThermoFisher Scientific, USA) and donkey anti-goat alexa fluor 680 (A21084, ThermoFisher Scientific, USA) secondary antibodies respectively. Images were taken with Lieca microsystems software (LAS AF lite version 2.6.0). 9 images

Copyright © 2018 by the American Thoracic Society

AJRCMB Articles in Press. Published on 12-June-2018 as 10.1165/rcmb.2018-0007OC

were taken per mouse and epithelial/ tight junction damage was scored by 4 blinded individuals using a scale from 0 to 3 where 0 = normal, organised epithelium with intact tight junctions, 1 = less organised epithelium, 2 = damaged epithelium and 3 = extensive damage to epithelium with few or no tight junctions.

Histological scoring of lung inflammation and fibrosis

Deparaffinised lung sections were stained with Haematoxylin (351945S, VWR, USA) and Eosin (341973R, VWR, USA) (H&E), Periodic Acid-Schiff (PAS) (102595, MP Biomedicals, USA and J/7300/PB08, ThermoFisher Scientific, USA) or Masson's Trichrome (HT10132, HT1079, HT151, HT153, B8563, Sigma-Aldrich, USA). To assess inflammation, each airway and blood vessel on H&E stained lung sections was assigned a score from 0 to 3 where a score of 0 is given to a bronchus or vessel not surrounded by any inflammatory cells and a score of 3 given when inflammation completely surrounds and is 5 or more cells in diameter from the edge of the bronchus or vessel. Average scores were then calculated for each lung section

For Masson's Trichome staining, levels of collagen staining and fibrosis in each lung section were assessed using the Ashcroft score system (Ashcroft et al., 1988).

Neutrophil chemotaxis

Lung tissue was disaggregated (see above) and passed through a cell strainer to obtain a single cell suspension. RBCs were lysed and remaining cells resuspended at a concentration of 5×10^6 cells / ml in RPMI 1640 medium (31870074, ThermoFisher Scientific, USA) containing 0.1% BSA (A2153, Sigma-Aldrich, USA). Chemotaxis plates (101-5, Neuroprobe, Inc., USA) were blocked with 30μl of RMPI

Copyright © 2018 by the American Thoracic Society

1640 medium containing 0.1% BSA for 30 minutes at room temperature before removal of this solution and addition of a recombinant hIL-8 concentration gradient (14-8089-80, ThermoFisher Scientific, USA) from 0 to 1000ng/ml. A filter was placed over the top of the chemokine solutions and 20μl of lung cells added to each one. Plates were incubated at 37 ^{o}C for 2.5h and the number of cells that had migrated into each well quantitated by addition of 30μl of CellTiter-Glo® Luminescent Cell Viability Assay reagent (G7570, Promega, USA) and reading on a TopCount.NXT™ luminescence counter (PerkinElmer Life and Analytical sciences, Italy).

Flow cytometry

A neutrophil oxidative burst assay using dihydrorhodamine 123 was performed using PBMCs and lung neutrophils. 2μl of a 5mM solution of DHR (D23806, Invitrogen Molecular Probes™, USA) were added to each sample and incubated at 37 ^{o}C for 5 minutes. Samples were washed once in PBS before data acquisition in channel FL-1 of a FACSCalibur (BD Biosciences, USA). For analysis of cell surface markers, phycoerythrin-conjugated anti-Gr1 (12-5931-82, eBioscience, Inc. USA), fluroescein isothiocynate-conjugated anti-CD18 (clone M18/2, MA1-10124, eBioscience, Inc. USA), and peridinin-chlorophyll protein/Cy5.5 conjugated anti CXCR2 (149307, BioLegend, USA) antibodies were used. All flow data was analysed with CellQuest software (BD Biosciences, USA).

***Pseudomonas aeruginosa* infection**

Mice were infected intranasally with 2x10^{6} CFU of *P. aeruginosa* (Xen41, Caliper Life Sciences, PerkinElmer, UK) in a volume of 40μl sterile PBS. Mice were culled for analysis at pre-defined experimental endpoints or when pre-defined humane

Copyright © 2018 by the American Thoracic Society

AJRCMB Articles in Press. Published on 12-June-2018 as 10.1165/rcmb.2018-0007OC

endpoints were reached. The relative quantity of *P. aeruginosa* in lung tissue was determined using SYBR Green (600828, Agilent, USA) and real time PCR primers specific for the *ecfX* gene (Clifford et al. 2012).

T cell assay

Mice were immunized sub-cutaneously in one hind footpad with 25μg of recombinant OprF protein (Quigley et al. 2015) emulsified with Hunters Titermax Gold adjuvant (T2684, Sigma-Aldrich, USA). At d10 the draining popliteal lymph node was harvested and disaggregated into a single-cell suspension for ELISPOT or for short-term culture with OprF antigen. CD4+ T cells responding to antigen were quantified by IFNγ ELISPOT (862.031.020, 2B Scientific, UK) performed in HL-1 serum-free medium (LZBE77201, Lonza, Switzerland), supplemented with L-glutamine (25030081, ThermoFisher Scientific, USA) and penicillin-streptomycin (15070063, ThermoFisher Scientific, USA). Cells ($2x10^5$) plus antigen were added to wells and incubated for 72h at 37^0C with 5% CO_2. Spots were counted on an automated ELISPOT reader (Autoimmun Diagnostika, Strasbourg, France).

Airway resistance and compliance (54-57)

Mice were anaesthetised by sub-cutaneous injection of 100μl of a 1:0.55:0.42 mixture of PBS, Medetomidine hydrochloride (Domitor®, Pfizer, USA) and ketamine (Ketaset®, Fort Dodge Animal Health Ltd, USA). After 15 minutes, a further 100μl of anaesthetic was administered by intra-muscular injection before cannulation of the trachea. Mice were placed onto an artificial ventilator and Resistance and Compliance measurements taken (Buxco, USA lung function equipment) in response

Copyright © 2018 by the American Thoracic Society

to PBS and increasing doses (3, 10, 30 and 100 mg/ml) of methacholine (A2251, Sigma-Aldrich, USA).

Measurement of bronchial hyperreactivity (Penh)

Measurement of bronchial hyperreactivity was performed by recording respiratory pressure curves by whole body plethysmography, calculated as Penh (Enhanced Pause, Buxco, USA). Mice were placed, fully conscious, into individual plethysmograph chambers and changes in air pressure between these chambers and a control chamber measured by a differential pressure transducer to give a lung function measurement for each individual mouse. Following a baseline measurement, Penh measurements were taken for each mouse in response to increasing doses (3, 10, 30 and 100mg/ml) of methacholine (A2251, Sigma-Aldrich, USA).

Isolation of airway smooth muscle (ASM) cells (58)

Lung tissue was chopped into approximately 1mm^2 pieces and incubated in 1ml DMEM media (32430-027, ThermoFisher Scientific, USA) containing 0.58 mg/ml Collagenase type D (11088858001, roche Diagnostics GmbH, Germany), 0.21 mg/ml Elastase (E7885, Sigma-Aldrich, USA), 0.83mg/ml bovine serum albumin (A2153, Sigma-Aldrich, USA) and 0.33 mg/ml Trypsin Inhibitor (17075029, ThermoFisher Scientific, USA) at 37^{0}C for 3h. Samples were washed once in media before placing lung pieces in a tissue culture plate with a small volume of DMEM containing antibiotics and 50% FCS. Cultures were left undisturbed for 3d and then media replaced and cells split as required. The phenotype of ASM cell lines was

Copyright © 2018 by the American Thoracic Society

AJRCMB Articles in Press. Published on 12-June-2018 as 10.1165/rcmb.2018-0007OC

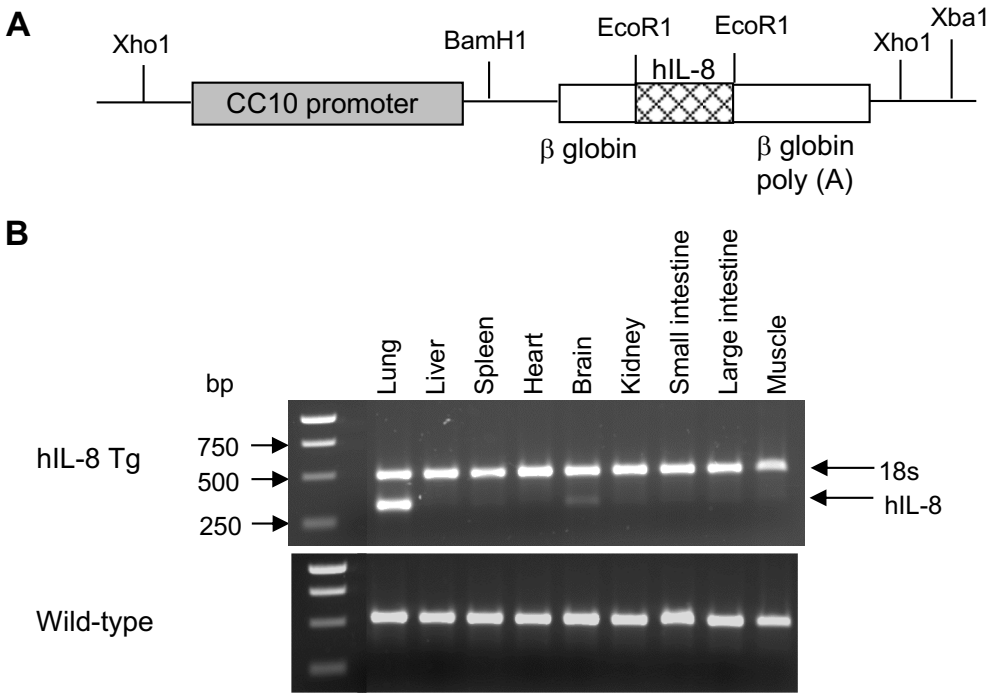
confirmed by light microscopy. In addition, cells were stained with antibodies against α-smooth muscle actin with omission of the primary antibody as a control.

Ca^{2+} Flux assays

Smooth muscle cells were resuspended in DMEM media containing 10mM HEPES (15630080, ThermoFisher Scientific, USA) and 2.5% FCS. Fluo-4 dye (F14201, Invitrogen, USA) was added to each cell suspension at a final concentration of 5μM and samples incubated for 45 minutes at 37 ^{0}C in the dark. Cells were washed once with DMEM and allowed to rest for 20 minutes at room temperature in the dark before stimulation. For each sample, a baseline measurement was acquired before rapid addition of the stimulant, calcium ionophore (A23187) (5μg/ml) (C7522, Sigma-Aldrich, USA) and continuation of data acquisition for at least 5 minutes. Data was acquired by continuous measurement in the FL-1 channel of a FACSCalibur (BD Biosciences, USA).

Copyright © 2018 by the American Thoracic Society

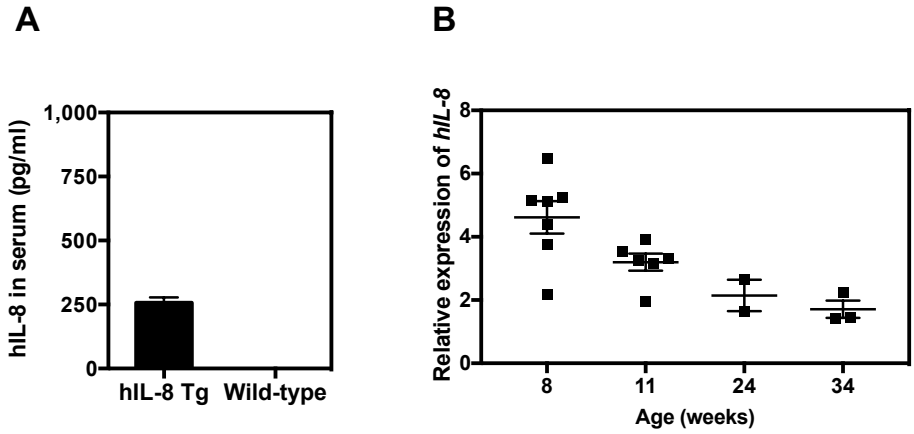
Supplementary Figure 1



Supplementary Figure 1. Generation of transgenic mice with lung targeted expression of hIL-8. (A) A DNA construct containing the coding sequence of hIL-8 under the control of the bronchial epithelial cell specific promoter, CC10, was injected into mouse oocytes. (B) RT PCR was used to detect cDNA transcripts for hIL-8 in lung samples from hIL-8 transgenic mice. With the exception of brain tissue, hIL-8 transcripts were not detected in any other tissue type. This data is representative of at least 3 animals per group.

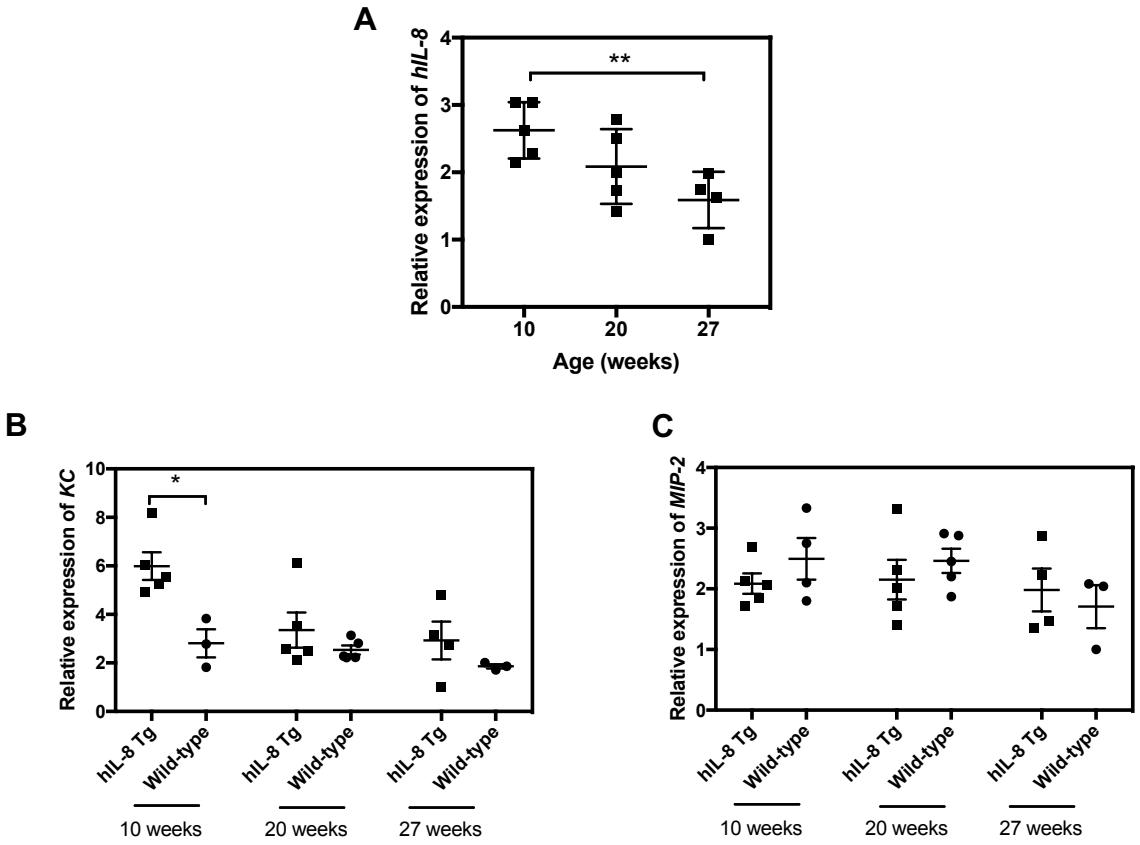
Copyright © 2018 by the American Thoracic Society

AJRCMB Articles in Press. Published on 12-June-2018 as 10.1165/rcmb.2018-0007OC



Supplementary Figure 2. A. Levels of hIL-8 protein in the serum of hIL-8 transgenic mice. B. Relative expression of hIL-8 in the lung of hIL-8 transgenic mice decreases with increasing age. (A) hIL-8 transgenic (black bars, n = 17) and wild-type mice (white bars, n=17). (B) RNA was extracted from the lung tissue of hIL-8 transgenic mice aged 8 weeks (n = 7), 11 weeks (n = 6), 24 weeks (n = 2) and 34 weeks (n = 3) and relative levels of hIL-8 transcripts determined by real-time PCR. Error bars represent mean ±SEM.

Copyright © 2018 by the American Thoracic Society



Supplementary Figure 3. Relative levels of *hIL-8*, *KC* and *MIP2* transcripts in the lungs of hIL-8 transgenic and wild-type mice at different ages. RNA was extracted from the lung tissue of hIL-8 transgenic mice aged 10, 20 and 27 weeks (n = 5, 5 and 4) and from wild-type mice of the same ages (n = 4, 5 and 3). Relative levels of (A) *hIL-8*, (B) *KC* and (C) *MIP2* transcripts were determined by real-time PCR. Error bars shown represent mean±SEM. Statistical significance was determined using an unpaired t-test (* $p<0.05$, ** $p<0.005$).

Copyright © 2018 by the American Thoracic Society

AJRCMB Articles in Press. Published on 12-June-2018 as 10.1165/rcmb.2018-0007OC

Supplementary table 1 – innate and adaptive array

Gene	p value	Fold-change
Ccl5	2.28E-04	3.74
Tlr6	7.49E-05	2.64
Il2	0.0129	2.44
Tbx21	0.004	2.18
Ifng	0.0041	1.73
Cd40	0.0000	1.69
Fasl	0.0194	1.69
Cd8a	0.0404	1.65
Irf7	0.0016	1.59
Il1b	0.012	1.59
Gata3	0.0002	1.58
Casp1	0.0047	1.54
Tnf	0.0153	1.5
Itgam	0.0076	1.48
H2-T23	0.0006	1.46
Cd4	0.0271	1.39
Slc11a1	0.0089	1.37
Stat1	0.0013	1.29
C5ar1	0.0137	1.28
Ifnar1	0.0243	1.25
Tlr9	0.0462	1.21
Tlr1	0.0001	-2.62

Copyright © 2018 by the American Thoracic Society

Supplementary table 2 – Fibrosis array

Gene	p value	Fold-change
Ccl3	0.0047	3.02
Fasl	0.0371	2.05
Ifnγ	0.0118	2.02
Il1β	0.0464	1.79
Cxcr4	0.0078	1.56
Bcl2	0.0256	1.39
Tgfb3	0.0378	1.35
Tgfbr1	0.0395	1.34
Tgfbr2	0.0381	1.32
Sp1	0.0444	1.2
Ltbp1	0.0486	-1.21
Timp1	0.0046	-1.55

Copyright © 2018 by the American Thoracic Society

AJRCMB Articles in Press. Published on 12-June-2018 as 10.1165/rcmb.2018-0007OC

Supplementary table 3 – Tight junction array

Gene	p value	Fold-change
Cldn4	0.012	2.83
Hcls1	0.01	1.67
Cldn8	0.024	1.58
Cldn3	0.045	1.48
Cldn10	0.005	1.48
Hsp90ab1	0.004	-1.22
Ctnna1	0.048	-1.24
Actn1	0.003	-1.24
F11r	0.029	-1.26
Cldn1	0.038	-1.3
Gnai1	0.046	-1.36
Cldn18	0.013	-1.4
Cgn	0.003	-1.41
Magi3	0.006	-1.44
Jam2	0.003	-1.67

Copyright © 2018 by the American Thoracic Society